

Consortium



for

Small-Scale Modelling

Technical Report No. 34

*COsmo Towards Ensembles at the Km-scale
IN Our countries (COTEKINO),
Priority Project final report*

May 2018

DOI: 10.5676/DWD_pub/nwv/cosmo-tr_34

Deutscher Wetterdienst

MeteoSwiss

Ufficio Generale Spazio Aereo e Meteorologia

ΕΘΝΙΚΗ ΜΕΤΕΩΡΟΛΟΓΙΚΗ ΥΠΗΡΕΣΙΑ

Instytucje Meteorologii i Gospodarki Wodnej

Administratia Nationala de Meteorologie

ROSHYDROMET

Agenzia Regionale Protezione Ambiente Piemonte

Agenzia Regionale Prevenzione Ambiente Energia Emilia Romagna

Centro Italiano Ricerche Aerospaziali

Amt für GeoInformationswesen der Bundeswehr

Israel Meteorological Service



www.cosmo-model.org

Editor: Massimo Milelli, ARPA Piemonte

COsmo Towards Ensembles at the Km-scale

IN Our countries (COTEKINO),

Priority Project final report.

Project participants:

*D. Alferov¹, M. Arpagaus², E. Astakhova¹, R. Bonanno³,
G. Duniec⁴, R. Keane⁵, W. Interewicz⁴, R. Kohlhepp⁵,
D. Leuenberger², N. Loglisci³, E. Machulskaya⁵, C. Marsigli^{6‡},
A. Mazur⁴, V. Maurer², A. Montani⁶, G. Rivin¹,
I. Rozinkina¹, L. Torrisi⁷, A. Walser²*

¹ Roshydromet

² MeteoSwiss

³ ARPA Piemonte

⁴ Instytucje Meteorologii i Gospodarki Wodnej

⁵ Deutscher Wetterdienst

⁶ Agenzia Prevenzione Ambiente Energia Emilia Romagna

⁷ Ufficio Generale Spazio Aereo e Meteorologia

[‡] Project Coordinator

Contents

1	Introduction	3
2	Initial Condition perturbations derived from KENDA	4
3	Model perturbations	4
3.1	Tests with the SPPT scheme	5
3.1.1	Tests at MCH	5
3.1.2	Tests at RHM	9
3.1.3	Tests at ARPA-SIMC	14
3.2	Test of the SKEB scheme in the 2.2 km ensemble at MCH	22
3.3	Information about improvements and a new strategy for model perturbations at DWD	23
4	Soil/surface perturbations	23
4.1	IMGW	24
4.1.1	Preliminary sensitivity tests	24
4.1.2	Extensive test-cases and sensitivity tests	29
4.1.3	Test-bed and configuration for (quasi-)operational EPS, concept of time-lagged ICs/BCs	35
4.2	ARPA Piemonte	43
4.2.1	Sensitivity of COSMO model to different lower boundary initial conditions.	43
4.2.2	Implementing a soil perturbation technique in a high resolution ensemble system.	47
5	References	49

Project leader

Chiara Marsigli (Arpa SIMC).

Contributing scientists

Dmitry Alferov (RHM), Marco Arpagaus (MCH), Elena Astakhova (RHM), Riccardo Bonanno (Arpa Piemonte), Grzegorz Duniec (IMGW), Richard Keane (DWD), Witold In-terewicz (IMGW), Regina Kohlhepp (DWD), Daniel Leuenberger (MCH), Nicola Loglisci (Arpa Piemonte), Ekaterina Machulskaya (DWD), Chiara Marsigli (Arpa SIMC), Andrzej Mazur (IMGW), Vera Maurer (MCH), Andrea Montani (Arpa SIMC), Gdaly Rivin (RHM), Inna Rozinkina (RHM), Lucio Torrisi (CNMCA), Andr Walser (MCH).

1 Introduction

In the recent years, more and more emphasis is being devoted to high-resolution rapid-update-cycle (RUC) NWP applications, since weather forecast is focusing more on high-impact weather (HIW) and small-scale intense phenomena (e.g. convection), also aiming at different applications (assistance to aviation, hydrology, civil protection). For this reason, NWP development is concentrating on high-resolution modelling, O(1km), and this is reflected in the COSMO strategy, which has lead to focusing the consortium development on high-resolution data assimilation, high-resolution modelling, high-resolution verification. Ensemble forecast was born to complement deterministic forecast, with products such as ensemble mean for medium-range predictions, ensemble spread to quantify the forecast uncertainty, meteograms for surface weather parameters, to present a spectrum of possible alternative scenarios. With the model resolution increase, the phenomena which are now described by NWP models are more and more stochastic in nature. For moist convection prediction, skill is manifested through the statistical properties of the forecasted convection instead of by deterministic modelling (Fritsch and Carbone 2004). Therefore, the weight given to ensemble forecast is now greater than it was some 10 years ago, since for the convection-permitting NWP models it is crucial to be able to forecast not only the “best scenario” but ideally the whole pdf or, more realistically, a good representation of it. The high-resolution of these systems prevents the possibility of running consortia ensembles, since it is prohibitive to cover a large domain with the required grid spacing. This is leading to the development of high-resolution ensembles on a national scale. Few years ago, DWD has started the development of a convection-permitting ensemble, COSMO-DE-EPS, which is operational over Germany at 2.8km horizontal resolution since May 2012 (Gebhardt et al., 2011). At the time of the COTEKINO PP, the system received initial condition perturbations from the 4 global scale operational analyses of DWD, ECMWF, NCEP and JMA. The four operational global runs of these institutions provides also boundary conditions to 4 COSMO runs at 7km horizontal resolution which drive in turn the COSMO-DE runs. Model physics perturbations are also applied, by changing the value of few parameters of the physics schemes. Then also Switzerland, Italy and Poland have started the development of convection-permitting ensembles in their countries. Furthermore, Russia has developed COSMO-RU2-EPS for assisting the Winter Olympics. Therefore, the need for a good strategy for convection-permitting ensemble has emerged at the Consortium level, requiring coordination among the activities taking place in the different countries, in order to share research and development work and to ensure good and timely exchange of in-

formation. This coordination has been organized through a Priority Project, COTEKINO (COsmo Towards Ensembles at the Km-scale IN Our countries). The COTEKINO Priority Project, which lasted for 2 years, was aimed at bringing to operations the COSMO ensemble forecasting systems for the convection-permitting scale. Several aspects of the design of convection-permitting ensembles have been taken into account, by organizing the Project in three Tasks: Initial Condition (Task 1, Section 2), Model perturbation (Task 2, Section 3) and Lower boundary perturbation (Task 3, Section 4). Boundary Conditions have not been considered in the Project. Anyway, a study about how to provide perturbed BCs to a convection-permitting ensemble has been carried out in Marsigli et al. (2014), showing that a direct nesting in a global ensemble of good quality may be a practicable solution, without the need of an intermediate step with a coarser resolution ensemble. The work carried out within the three Tasks is presented in the following Sections of this Report.

2 Initial Condition perturbations derived from KENDA

It is recognised that for the forecasting horizon of the convection-permitting ensembles, data assimilation plays a crucial role. What dominates ensemble spread in the first six hours are perturbed initial conditions (Peralta et al, 2012, Vié et al, 2011), which should include both a good estimate of the initial condition(s) and a good representation of its (their) uncertainties. Within the KENDA PP, a LETKF scheme for the km-scale has been developed, aiming at providing both deterministic analysis for driving high-resolution COSMO runs and a set of perturbed analyses to drive high-resolution ensembles. Though the KENDA development is included in the KENDA PP, how to set-up the system to provide ICs to a convection-permitting ensemble and how to derive ICs from KENDA was addressed in the COTEKINO PP. In particular, it was organised the communication about experiments and their results, the exchange of dedicated tools and the coordination with the KENDA PP itself. This activity has been carried out by Chiara Marsigli and Tiziana Paccagnella (ARPA-SIMC), Daniel Leuenberger and André Walser (MeteoSwiss), Richard Keane (DWD), from the COTEKINO PP side and by Christoph Schraff, Hendrik Reich and Roland Potthast (DWD) from the KENDA side. The coordination has been performed mainly thanks to meetings organized jointly with KENDA PP (COSMO GM 2014, CUS 2015). Results have been presented and discussed and further experiments have been agreed and planned. Tools for diagnostics have also been shared.

3 Model perturbations

The importance of model perturbations in ensemble forecasting has been recognised since some years. It is found that model perturbations usually play a smaller role with respect to initial conditions (at the beginning of the run) and boundary conditions (later) perturbations, but they may become crucial in specific weather situation (Marsigli et al, 2009; Gebhardt et al, 2011) and a poor representation of the model error may lead to severe underestimation of the ensemble spread (Vié et al., 2011). Several techniques have been developed to represent model error: perturbation of the physics schemes parameters (Marsigli, 2009; Gebhardt et al, 2011), random parameters (Bowler et al, 2008), SKEB (Shutts, 2005; Berner et al., 2009), SPPT (Buizza et al, 1999; Palmer et al, 2009), multi-physics, stochastic physics (Plant and Craig, 2008; Bengtsson et al., 2013). Interesting comparative studies have also been carried out (Berner et al, 2011; Hacker et al, 2011). While there are some results about the applicability of these techniques for the O(10km) scale, it is still not assessed how to use them for the O(1km) scale. From the COSMO-DE-EPS experience it is clear

that underdispersion severely affects the ensemble for surface variables, if only few physics parameters are perturbed. The SPPT scheme of ECMWF has been implemented in the COSMO code, to test its capability of representing model error in the LETKF ensemble. This code can be tested also for the ensemble forecasting set-ups, though it is argued that this approach may lead to serious unbalances in the model. Also, the scheme has been originally developed for the IFS model at coarser resolution and should be adapted for use at the $O(1\text{km})$ scale. On top of this, the SKEB scheme has been implemented in the COSMO model, opening the possibility of testing this approach for providing model perturbations to the convection-permitting ensembles. Finally, DWD has started the development of a new approach for model perturbation, aiming at simulating the model error as a continuous stochastic process with the same statistically properties as the empirically determined error of model tendencies.

3.1 Tests with the SPPT scheme

3.1.1 Tests at MCH

At MeteoSwiss, the SPPT scheme has been tested for the ensemble prediction system COSMO-E with 21 members for the Alpine area (see Fig. 1) and a mesh-size of 2.2 km and 60 model levels. The implementation of the SPPT in the COSMO code has been done by Lucio Torrisi and has been used in our first study to find an appropriate SPPT setup for the convection-resolving resolution as well as to understand the impact of the scheme on spread and error of temperature and humidity in COSMO-E. The main findings are:

- larger random numbers produce larger spread and faster spread growth
- larger correlation-lengths in space and time for the random numbers lead to substantially larger spread
- the spread increase due to SPPT decreases with increasing height above the surface

Details about this first study are given in Maurer et al. (2014).

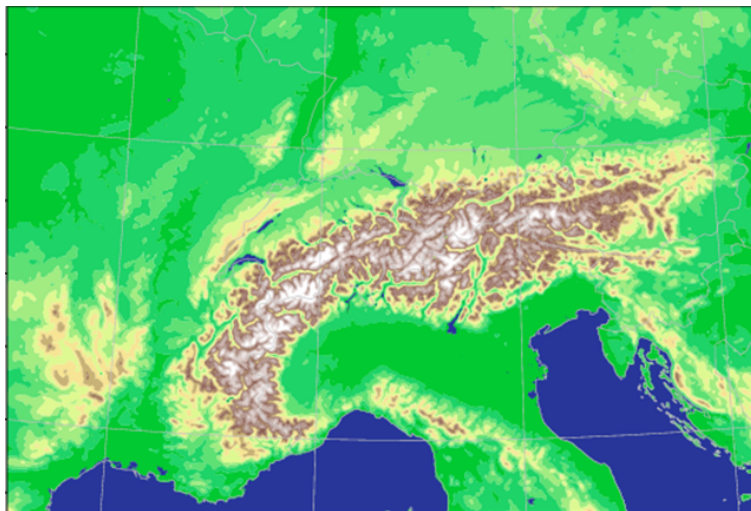


Figure 1: COSMO-E model domain for the experiments with orography.

In the course of the study, the SPPT implementation in COSMO has been reviewed and improved. In particular, perturbing the tendencies of the Coriolis force has been removed

as well as a few technical changes has been done to support single precision and to ensure the same results with different compilers. The revised SPPT code has been integrated into the official COSMO version 5.1. Further experiments for a summer period confirm these results and demonstrate that turning off the SPPT tapering below 850 hPa does not cause model stability problems and significantly increases the spread in the planetary boundary layer. Furthermore, deterministic forecasts for a summer and winter month in 2012 show no significant quality degradation with SPPT, even for rather strong stochastic perturbations of physical tendencies. Therefore, an aggressive SPPT parameter setting has been chosen for COSMO-E with:

- `itype_vtaper_rn=2`
- `itype_qxpert_rn=1`
- `itype_qxlim_rn=0`
- `hinc_rn=6`
- `dlat_rn/dlon_rn=5.0`
- `stdv_rn=1.0`
- `range_rn=0.9`
- `lgauss_rn=.TRUE.`
- `lhorint_rn/ltimeint_rn =.TRUE.`

This setup is used for further experiments to investigate the spread-error relationship in detail. To this end, 00 UTC COSMO-E forecasts are run for every second day from 26 July to 25 August 2012 for a summer period and from 3 December to 31 December 2012 for a winter period. Initial conditions including perturbations (if used) are taken from an early KENDA assimilation cycle in test mode which has been implemented at MeteoSwiss, while IFS-ENS control and members 1-20 are used to drive the COSMO-E forecasts at the lateral boundaries. The experiments are run with COSMO v5.0 including local modifications and with single precision (Rüdisühli et al., 2014). According to Jolliffe et al. (2011) the standard deviation of the ensemble mean error (STDE) needs to match the root mean ensemble variance (RMEV) for a reliable forecast. This is further discussed in Maurer et al. (2014). Fig. 2 shows RMEV (spread) and STDE (error) with respect to analysis for experiments without initial condition perturbations for temperature at the lowest model level, which is about 10m above surface. For summer, RMEV is clearly smaller than STDE in the first 4 days (i.e. roughly up to lead-time +96h) without SPPT and SPPT reduces the gap between RMEV and STDE to a large extent mainly by augmenting the daily cycle of RMEV. For the winter period, RMEV is clearly smaller than STDE in the first 3 days (i.e. roughly up to lead-time +72h) and the increase in RMEV due to the SPPT is much smaller. In the middle and upper troposphere the RMEV matches the STDE quite well except for the first day, also for the experiments with initial condition perturbations (not shown).

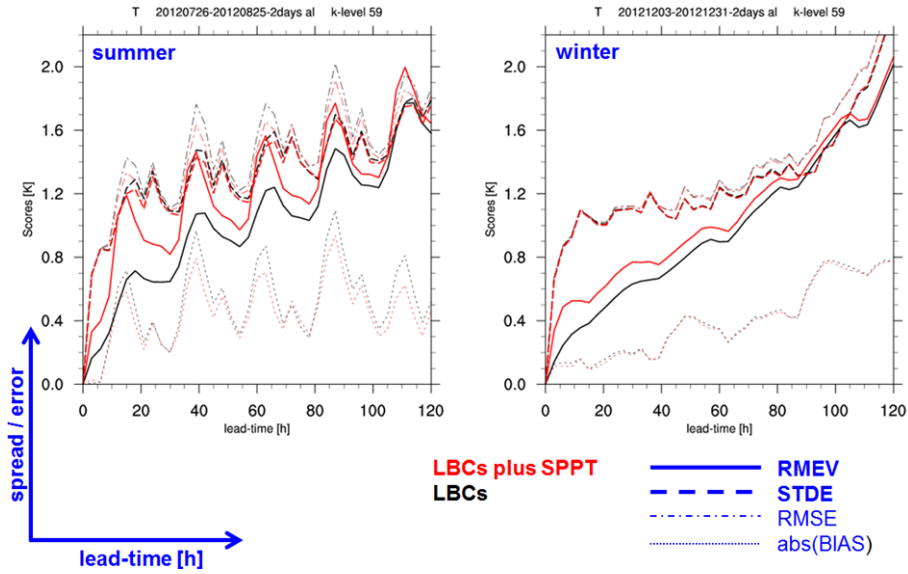


Figure 2: Root-mean ensemble variance (RMEV; bold solid), standard deviation of ensemble mean error against analysis (STDE; bold dashed), root mean square error of ensemble mean (RMSE; dashed-dotted) and the absolute value of the bias (dotted) for temperature as a function of forecast lead-time on the lowest model level at about 10m above surface averaged over the model domain for a summer (left) and winter (right) period without initial condition perturbations and with two different setups: boundary condition perturbations plus SPPT (red) and boundary condition perturbations only (black).

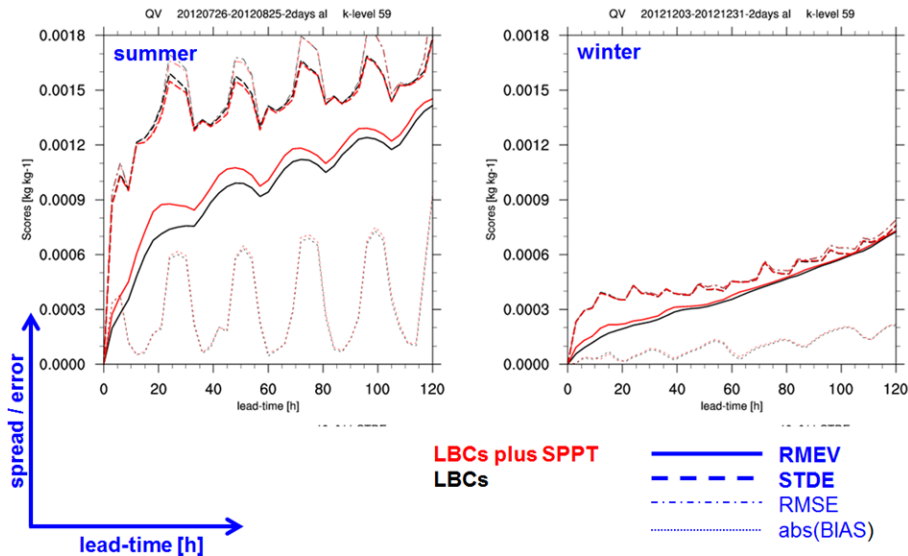


Figure 3: As Fig. 2 but for specific humidity.

Similar results are found for wind speed (not shown) but the underdispersiveness in winter with SPPT is clearly smaller than without. In contrast, the underspersiveness for specific humidity is much larger and SPPT does only slightly reduce the large gap between RMEV and STDE both in summer and winter (see Fig. 3). In the following, the vertical structure of the impact of SPPT is discussed for the summer period. Fig. 4 shows the RMEV, STDE, BIAS and RMSE differences for temperature between the summer experiments with and without SPPT for all model levels as a function of lead-time. The impact for temperature has an obvious daily cycle and is significant up to about level 42, i.e. up to about 2500m

above surface. Interestingly, SPPT does not only increase spread, it also decreases BIAS and STDE slightly (and thus RMSE as well). Similar results are found for wind speed and specific humidity in terms of RMEV, but the impact of SPPT clearly decreases with increasing lead-time (not shown).

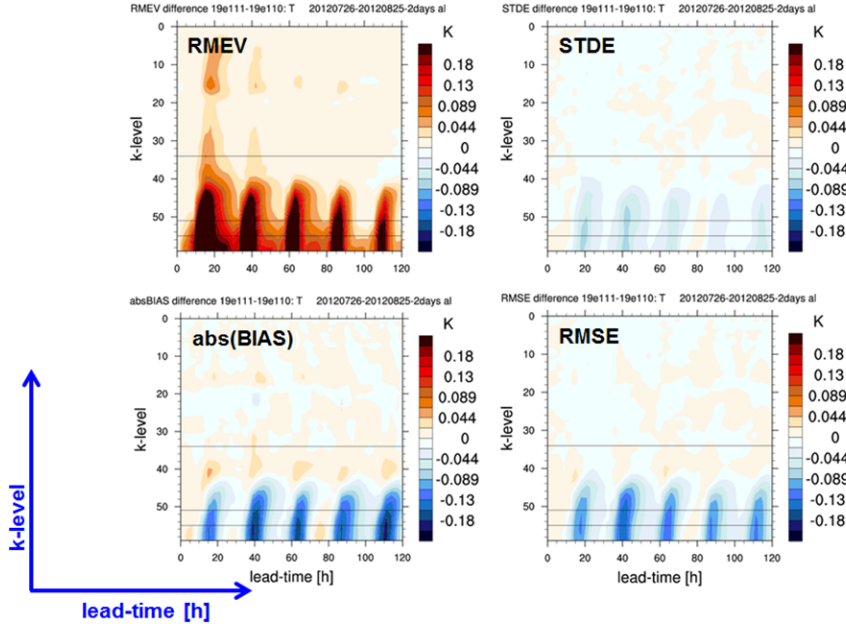


Figure 4: Difference between experiments with and without SPPT for RMEV (top left), STDE (top right), abs(BIAS) (bottom left), and RMSE (bottom right) for temperature on all model levels as a function of forecast lead-time for the summer period. The experiments use initial and lateral boundary condition perturbations.

In order to better understand the impact of SPPT, the tendency contributions from the different parametrizations are investigated. In the COSMO-E setup, the following parametrizations contribute to the sum of the temperature tendencies which is then perturbed by SPPT: turbulence, microphysics, shallow convection, and radiation. Fig. 5 shows the contribution of the different parametrizations on all model levels as a function of lead-time for a summer and winter day. It points out that for the summer day the tendencies from the turbulence scheme are at least an order of magnitude larger than the other ones. The tendencies show a daily cycle with values largest near-surface. This explains well the daily cycle of the SPPT impact on near-surface temperature in the summer period. For the winter day, the tendencies from the turbulence and radiation scheme are naturally smaller which explains the smaller impact of SPPT in winter. For the chosen day, they are of the same order of magnitude as the microphysics tendencies.

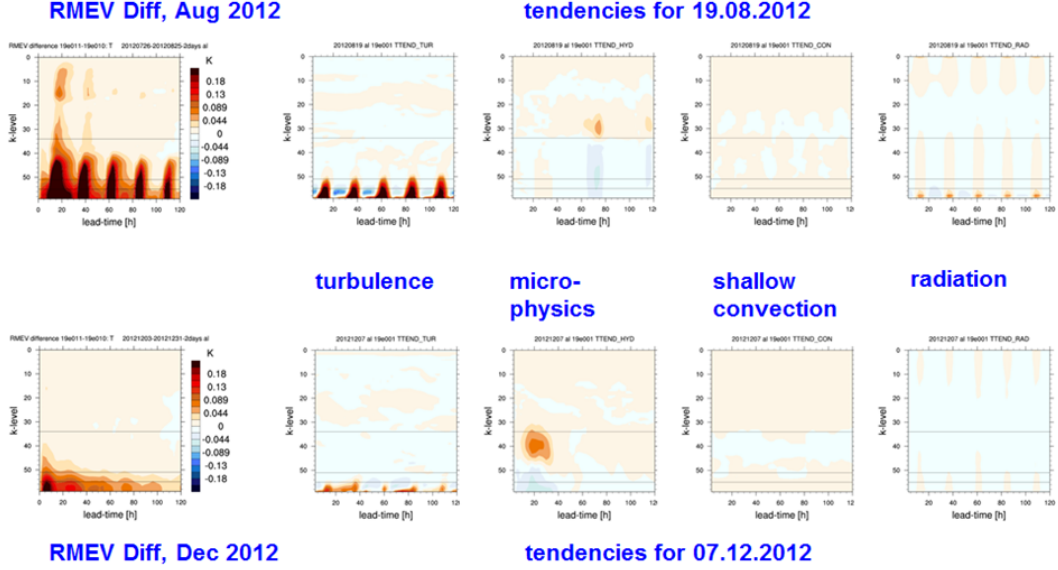


Figure 5: RMEV for temperature for the summer (top left) and winter (bottom left) period and temperature tendencies of the turbulence, microphysics, shallow convection and radiation scheme on all model levels as a function of lead-time for a summer (top) and winter (bottom) day. The sum of these temperature tendencies is perturbed by SPPT.

A further study has investigated the impact of an overlaid second smaller-scale spatial SPPT pattern and the impact of soil moisture perturbations. Both experiments show a positive impact for a summer case by further increasing the spread. However, they have only limited impact in winter when additional spread would be most helpful since then SPPT is less effective in representing model errors. In summary, the COSMO-E experiments show, primarily in summer, a significant improvement of RMEV, STDE, and BIAS due to SPPT in the lower troposphere for the entire forecast range, but they still lack spread in the first 3 days, in particular for humidity. In the middle and upper troposphere the experiments generally show a satisfactory spread-error relation, with the poorest results again for humidity which shows rather too little spread also at upper levels. The tendencies from the turbulence scheme generally show the largest physics tendencies and hence contribute strongest to the SPPT impact.

3.1.2 Tests at RHM

The goal of the RHM research was to assess the effect of stochastic perturbation of physical tendencies with different parameter settings in COSMO-Ru2-EPS (Montani et al., 2014). The ensemble consisted of 10 members, run with the COSMO model with a horizontal resolution of 2.2 km and 50 levels in vertical. The integration domain was the Sochi area. The initial and boundary conditions were provided by COSMO-S14-EPS (Montani et al., 2013). The period from 1 to 28 February 2014 was considered. The forecast length was 48h. The operational forecasts issued twice a day (00 and 12 UTC) during the Sochi Olympic Games 2014 were used as a reference experiment named noSPPT hereafter. The reference runs were carried out with COSMO model version 4.22. A set of experiments with COSMO-Ru2-EPS (the same EPS setting and period as in the reference experiment but model version 5.01) with different SPPT settings was held. The list of experiments and the corresponding SPPT settings are given in Table 1. In all experiments the distribution of random numbers was Gaussian (lgauss_rn=true., default); a 5 deg x 5 deg coarse grid was used for random numbers (dlat_rn=dlon_rn=5); the random number field was changed every 6 hours (hinc_rn=6,

default); the tapering was prescribed by default near the surface and in the stratosphere (`itypevtaperrn=1`), and only one random number pattern with its correlation scales was applied (`npattern_rn=1`, default). The following SPPT parameters were varied:

- the standard deviation of the Gaussian distribution of random numbers `stdv_rn`;
- the upper limit imposed to the absolute value of random numbers `range_rn`;
- the parameters showing whether the random numbers are interpolated in space `lhorint_rn` and time `ltimeint_rn`;
- the parameter `itype_qxpert_rn`, showing which hydrometeor tendencies are perturbed;
- the parameter `itype_qxlim_rn`, determining the type of reduction/removal of the perturbation in case of negative or supersaturated values of specific water vapor content or negative other water-content related characteristics.

All SPPT runs completed successfully with no numerical instabilities. Both case study evaluation and probabilistic verification of monthly series of forecasts were carried out. The results of experiments SPPTtest and noSPPT were compared for the two cases: the tropospheric föhn event on February 7, 2014 and the heavy precipitation event on February 18, 2014. It was found that the SPPT effect on 2m T ensemble spread depends on orography (see Fig. 6). With SPPT the spread strongly increased over high mountains, moderately grew over low regions (including sea), and decreased over areas of medium heights. The strongest increase in the ensemble spread over high domains can be considered as a positive effect of SPPT introduction because the temperature forecasts above 1500 m were poor during the föhn (thus higher spread corresponded to less skilful forecast).

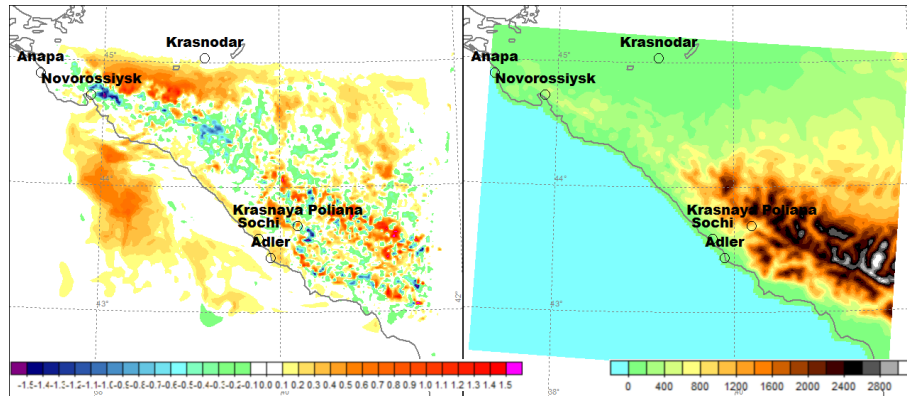


Figure 6: Left panel: difference of 2m temperature ensemble spread in experiments with and without SPPT (SPPTtest minus noSPPT). 30-h forecast starting at 00 UTC on February 6, 2014. Right panel: model orography.

For the case of heavy precipitation on February 18, 2014, the system with SPPT was more skilful in predicting the rain start. Also, it gave less false heavy rain areas and more correct peaks. However, the location of maximum precipitation was better predicted in the noSPPT experiment.

Perturbed parameters	Experiment name and SPPT settings						
	noSPPT	SPPTtest	SPPTphys	SPPTinphys	SPPT_W	SPPT_W + phys	SPPT_W + intphys
stdv_rn			0.4			1.0	
range_rn			0.8			0.9	
lhorint_rn	N\A	.FALSE. (no interpolation of perturbations)	.TRUE. (interpolated perturbations)	.FALSE. (no interpolation of perturbations)	.TRUE. (interpolated perturbations)		.TRUE. (interpolated perturbations)
itimeint_rn		0 (q_v only)	2 ($q_v, q_c, q_i, q_r, q_s, q_g$)				
itype_qxpert_rn		0 (no limitations imposed)	1 (do not perturb tt T- and tt q_v tendencies if new q_v are negative or supersaturated)	0 (no limitations imposed)	1 (do not perturb tt T- and tt q_v tendencies if new q_v are negative or supersaturated)		

Table 1: List of experiments with COSMO-Ru2-EPS and corresponding SPPT settings.

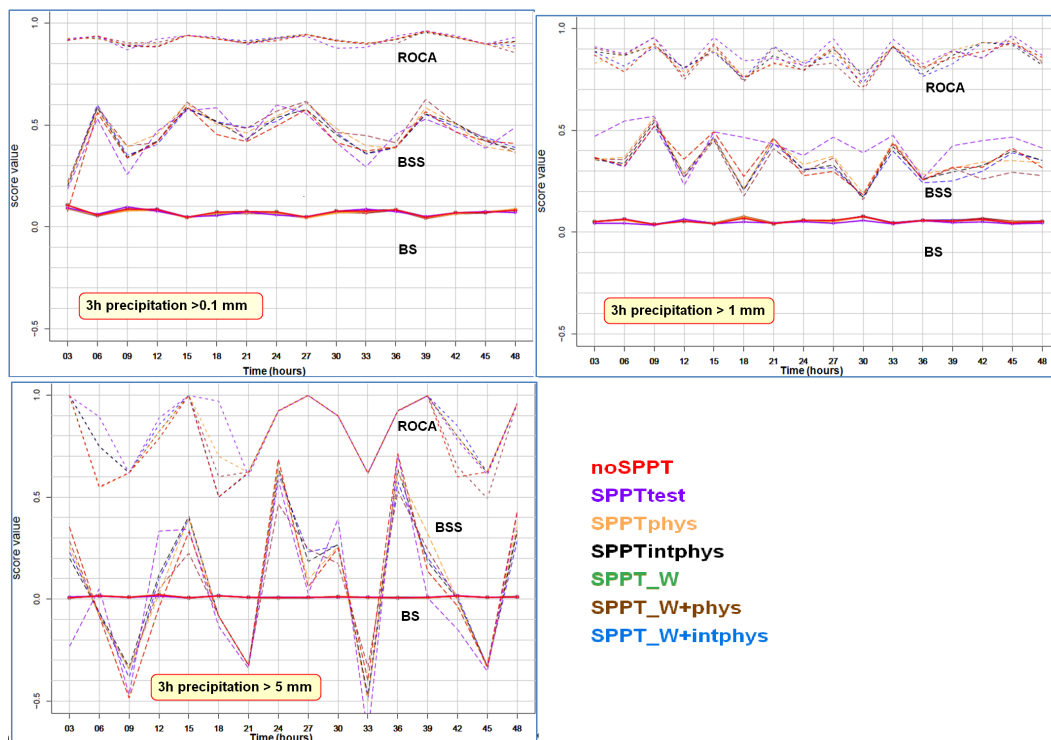


Figure 7: Verification of precipitation forecasts for various SPPT parameter settings.

The probabilistic verification was performed for the monthly (February 2014) series of COSMO-Ru2-EPS forecasts (56 in total, with no regard for the initial forecast time). The Brier score (BS), the Brier skill score (BSS) and the area under the ROC curve (ROCA) were computed for 3-hour total precipitation sum, 2-m air temperature, and 10-m wind speed. The verification was against observations at 31 meteorological stations in the Sochi region (<http://frost2014.meteoinfo.ru>). R-based utilities developed and kindly provided by A. Muravev were applied. Some positive effect of using SPPT was found for precipitation forecasts, especially for the event “3-h precipitation is greater than 1 mm”. Though the application of different SPPT settings resulted in very close scores, SPPTtest was undoubtedly the best for the thresholds of 1 mm/3h and 5 mm/3h (Fig. 7). As for the 2-m temperature forecasts, SPPT did not improve their skill (Fig. 8). The experiment noSPPT was the best especially for high thresholds. SPPTtest, which demonstrated the best precipitation forecasts, was the worst in terms of 2-m temperature forecasts. Generally, the probabilistic scores for temperature differ more between the experiments than for precipitation. However, no sensitivity was found to interpolation of random numbers (parameters `lhorint_rn`, `ltimeint_rn`) and to the method applied to avoid problems with negative or supersaturated water vapor values (parameter `itype_qxlim_rn`). The verification results demonstrated the advantage of perturbing all hydrometeor tendencies and using wider distributions of random numbers.

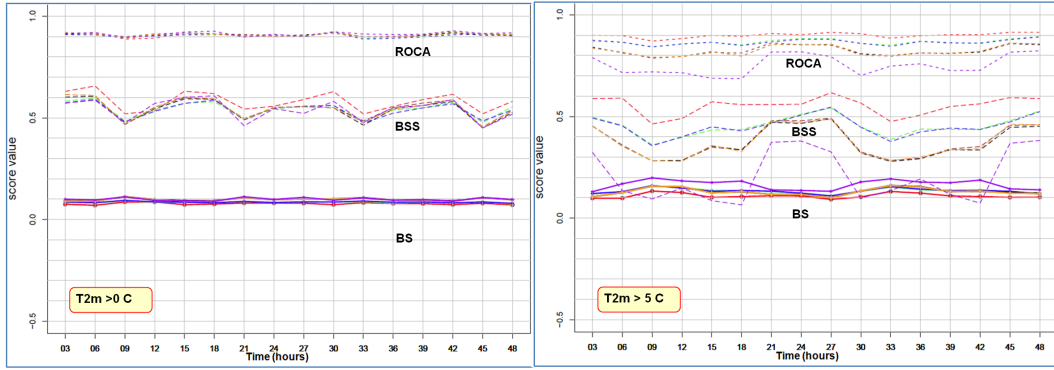


Figure 8: The same as Fig. 3 but for 2-m temperature.

The introduction of SPPT not only affected the probabilistic scores but also led to temperature biases that vary depending on the SPPT settings. Fig. 9 shows the monthly-averaged errors of the ensemble mean for different experiments at the Krasnaya Polyana station.

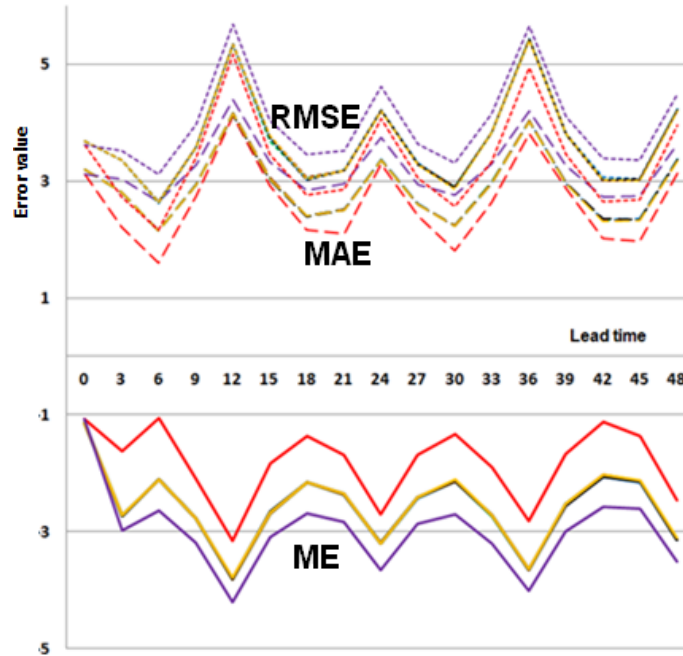


Figure 9: Mean error (ME, solid), mean absolute error (MAE, long-dashed), root-mean-square error (RMSE, dashed) for 2m T ensemble mean forecasts at Krasnaya Polyana station. Experiment as in Fig. 7.

The plot confirms the superiority of experiments with higher standard deviation of random number distribution and perturbation of all hydrometeor tendencies. High sensitivity of 2m T forecast skill to SPPT settings indicates that they could be improved as a result of SPPT tuning. Though SPPT seems to introduce biases to 2m T forecasts, it can improve the temperature distribution. The forecast histogram for experiment with SPPT in Fig. 10 looks more like the observation histogram than that for the experiment without SPPT.

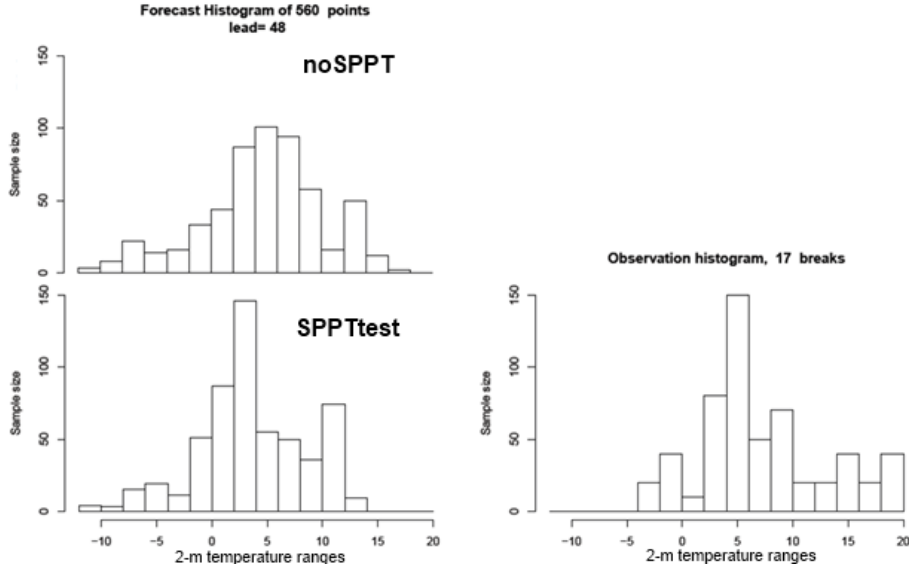


Figure 10: 2m T distribution histograms for noSPPT and SPPTtest 48-h forecasts and for observations at Krasnaya Polyana. February 1-28, 2014.

Wind speed forecast scores were rather poor both with and without SPPT. SPPT settings did not make significant difference.

Conclusions

Case studies in the Sochi mountainous area with COSMO-Ru2-EPS demonstrated that SPPT could be useful for precipitation forecasts, slightly improving the description of rain localization and start. The SPPT-related spread of 2m T ensemble forecasts correlates with the model orography. SPPT additional spread amplifies the coincidence between high-spread areas and the areas of less skilful forecast. The probabilistic verification of monthly series of COSMO-Ru2-EPS forecasts (56 in total) demonstrated a positive effect of using SPPT for precipitation forecasts, especially for the event “3-h precipitation is greater than 1 mm”. Variations in the SPPT settings did not influence the results for precipitation much. SPPT worsens the 2m T forecasts, introducing temperature biases and deteriorating probabilistic scores. The verification showed rather large differences between the skills of experiments with various SPPT settings. At the same time, the eyeball analysis showed that the predicted temperature distribution became more realistic when physical tendencies were perturbed. Therefore, SPPT did not add value to temperature forecasts, but can sometimes improve the representation of distribution. It is possible to improve the 2m T forecast by varying the SPPT settings. For example, in most cases perturbations of all hydrometeor tendencies lead to better results than perturbations of specific water content tendency only. Also the increase of the range of standard deviation for the Gaussian distribution of random numbers and of the upper limit imposed to the absolute value of random numbers positively contributed to the results.

3.1.3 Tests at ARPA-SIMC

At ARPA-SIMC the SPPT scheme has been tested both in the COSMO-LEPS ensemble and in the COSMO-IT-EPS ensemble.

COSMO-LEPS

In the framework of the experimentation carried out in the PP, COSMO-LEPS was run for

Variables	2-m temperature, 10-m wind speed, 12-h cumulated precipitation
Period	22/11/2014 - 31/01/2015, starting at 12UTC
Verification period	35-55N, 0-20E (about 1000 synop reports/day)
Thresholds (for precipitation only)	1, 5, 10, 15, 25, 50 mm/12h
Method	Nearest grid point
Systems	OPER-CLEPS (v5.0) and SPPT-CLEPS (v5.1)

Table 2: Main features of the verification configuration.

about 70 days with SPPT switched on (SPPT-CLEPS) and its performance was compared to the operational set-up (OPER-CLEPS) for a number of surface variables. The verification network is provided by the synop reports which fall inside a domain covering Central and Southern Europe. On average, about 1000 observations are available for verification at each forecast range (Fig. 11).

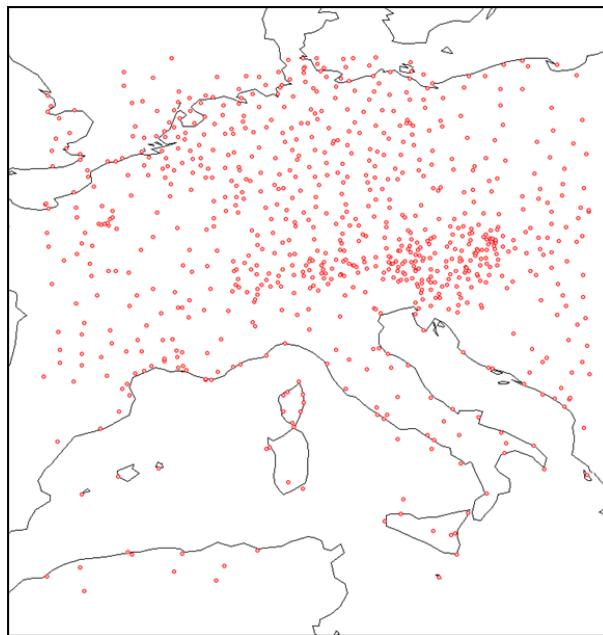


Figure 11: The verification domain used for inter-comparison between OPER-CLEPS and SPPT-CLEPS.

Table 2 summarises the main features of the experimentation.

As for the verification of temperature and wind-speed, the attention is focussed on the spread/skill relation of the two systems. As reported in Fig. 12, SPPT-CLEPS (blue lines) presents a larger spread than OPER-CLEPS for all forecast ranges. This is especially true for wind-speed and less evident for temperature. On the other hand, the impact on the forecast skill of the ensemble mean is negligible. In either cases, there is still a lack of spread in the short range, although the use of SPPT partly mitigates the underdispersion problem of COSMO-LEPS.

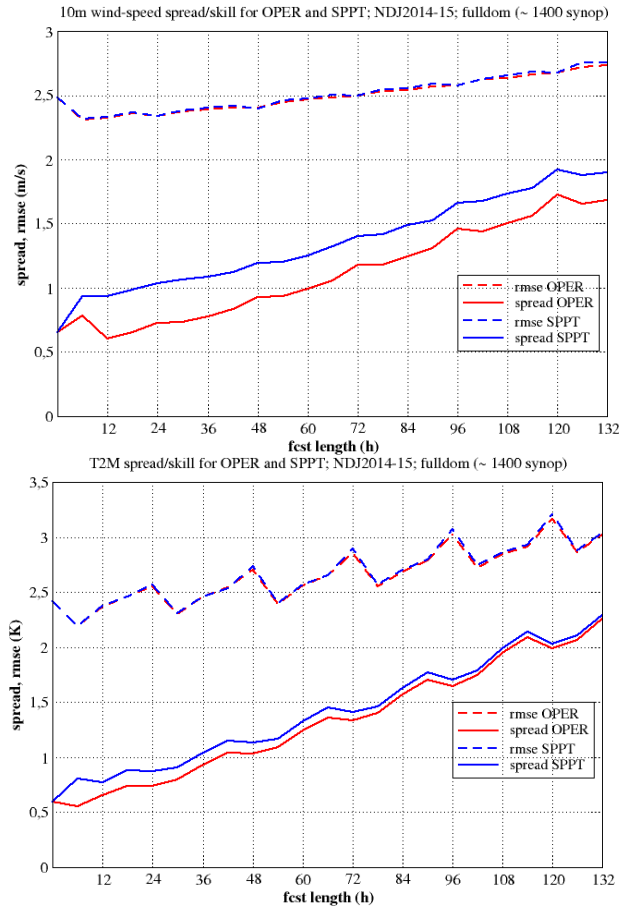


Figure 12: Spread/skill relation of OPER-CLEPS (red) and SPPT-CLEPS (blue) in terms of 2-m temperature (top panel) and 10-m wind speed (bottom panel) as a function of the forecast range. The rmse of the ensemble mean (spread) is reported as dashed (solid) line.

As for precipitation, the attention is focussed on the probabilistic prediction of 12-hour cumulated precipitation. In particular, the attention is focussed on the predictive skill of both systems for 2 types of events: 12-hour precipitation exceeding 1 mm and 10 mm. The left (right) panel of Figure 13 reports the values of the ROC area as a function of the forecast range for the 1mm (10 mm) threshold.

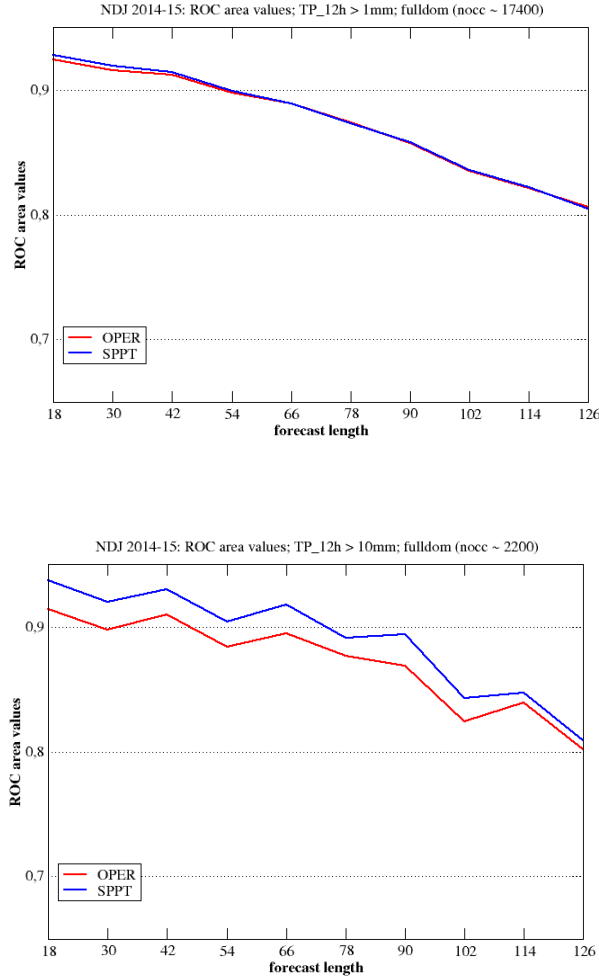


Figure 13: Roc area values for OPER-CLEPS (red) and SPPT-CLEPS (blue) as a function of the forecast range for the events: total precipitation over 12-hour exceeding 1 mm (top panel) and 10 mm (bottom panel).

It can be noticed that for the lower threshold, with about 17400 occurrences over the verification period of Table 2, the performance of OPER-CLEPS and SPPT-CLEPS is almost identical. On the other hand, for the higher threshold (about 2200 occurrences), some positive impact of using SPPT can be noticed. Therefore, on the basis of these encouraging results, it is planned to carry on the experimentation and assess the benefits of using SPPT also during summer months. In addition to that, it is also envisaged to study the possibility to run SPPT-CLEPS in single-precision mode, thus saving about 30% of computing resources and enabling the implementation of a larger-size COSMO-LEPS.

COSMO-IT-EPS

The COSMO-IT-EPS ensemble is an experimental convection-permitting ensemble running over Italy over selected cases/periods, aiming at the definition of an ensemble set-up to be operationally implemented as part of the Italian modelling chain. The COSMO model is run at 2.8 km of horizontal resolution, with 50 vertical levels, on an Italian domain. The ensemble has 16 members, which receive Initial and Boundary Conditions from the members of COSMO-LEPS. The aim of this work was to study the role of the physics perturbations focusing on severe rainfall events occurred in Italy. Three experimental ensemble set-ups

were run:

- no model perturbation (downscaling)
- perturbation of few physics parameters (PP)
- stochastic perturbation of physics tendencies (SPPT)

Two main rainfall events occurred in Italy in autumn 2014 were selected:

- Genova event, 9 October 2014
- Parma event, 13 October 2014

For the Genova event, the 6h accumulated precipitation estimated by radar during the 9th of October are shown in the first row of Fig. 14, while in the second row is shown the precipitation forecasted over the same time periods by the COSMO-I2 operational deterministic run.

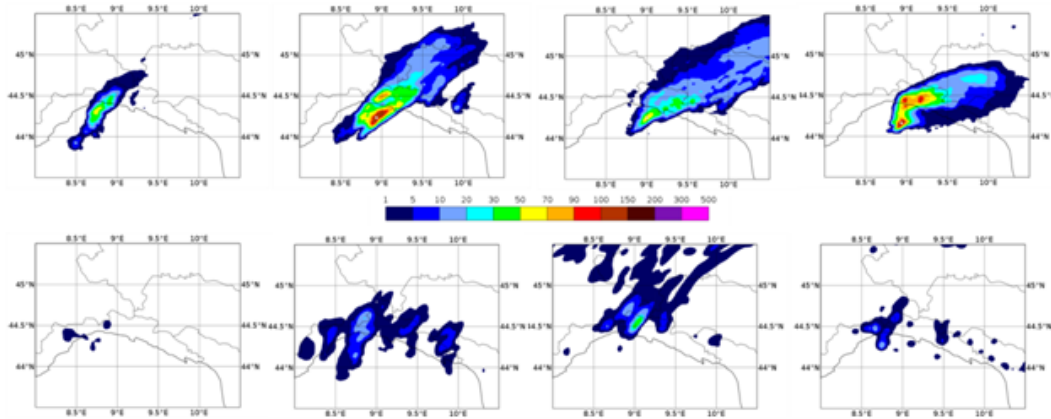


Figure 14: 6h accumulated precipitation during the 9th of October as estimated by radar (top row) and as forecasted by the COSMO-I2 operational deterministic run (bottom row).

For the Parma event, the precipitation accumulated over 24 hours, as measured by raingauges is shown in the left panel of Fig. 15, while in the right panel is shown the precipitation forecasted by the deterministic COSMO-2I model. The areas of maximum observed precipitation are highlighted in both plots by coloured ellipses.

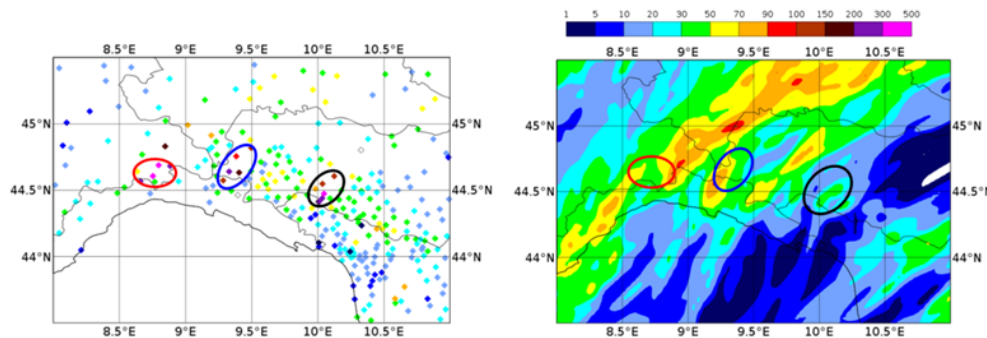


Figure 15: 24h accumulated precipitation during the 13th of October as measured by raingauges (left panel) and as forecasted by the COSMO-I2 operational deterministic run (right panel).

For the Genova event the behaviour of the 3 experimental suites is shown in the following figures, focussing on the 6h where the heaviest precipitation was observed, between 18 and 24 UTC of the 9th of October. In each figure, the precipitation forecasted by each ensemble member is shown, as well as the radar estimate in the uppermost right panel. In general, the ensemble members are able to forecast intense precipitation in the selected 6h period, but they tend to shift the structure toward the west (Fig. 16). The addition of parameter perturbations (PP, Fig. 17) permits to increase the diversity between the members and the introduction of the SPPT perturbation (Fig. 18) brings on top an enhancement of the precipitation forecasted by some members.

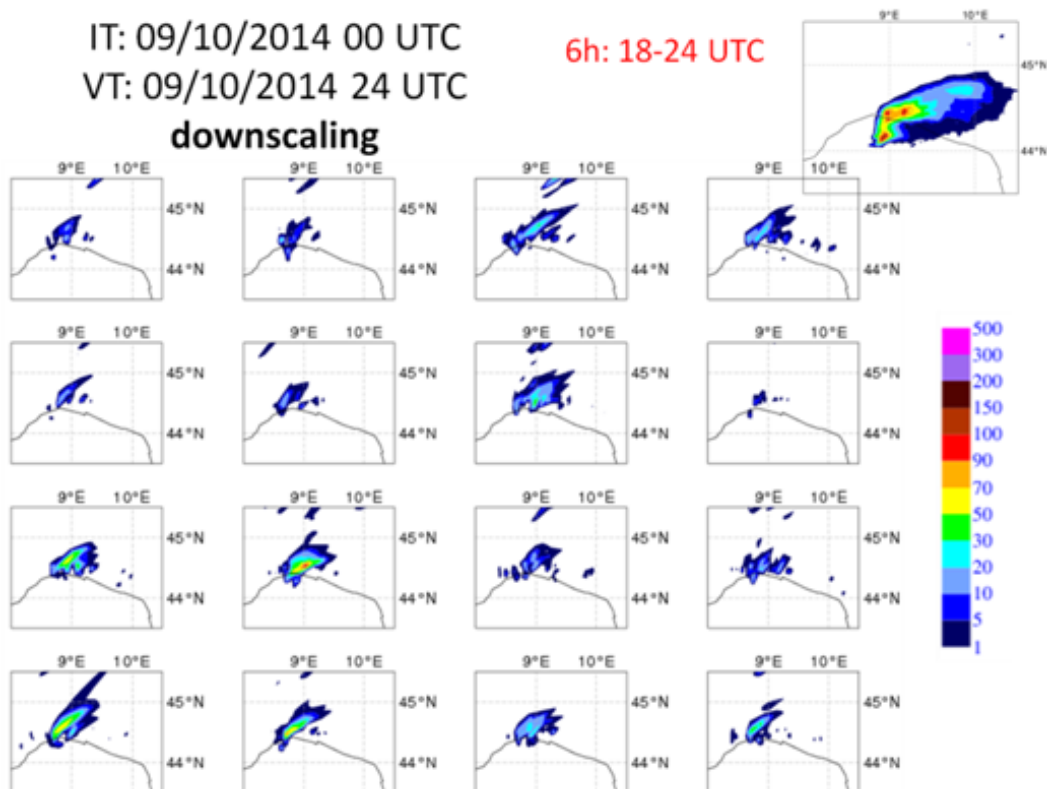


Figure 16: In the panels is shown the precipitation forecasted by each member of the downscaling ensemble accumulated over the 6 hours between 18 and 24 UTC of the 9th of October. The radar estimate for the same period is also shown in the uppermost right panel.

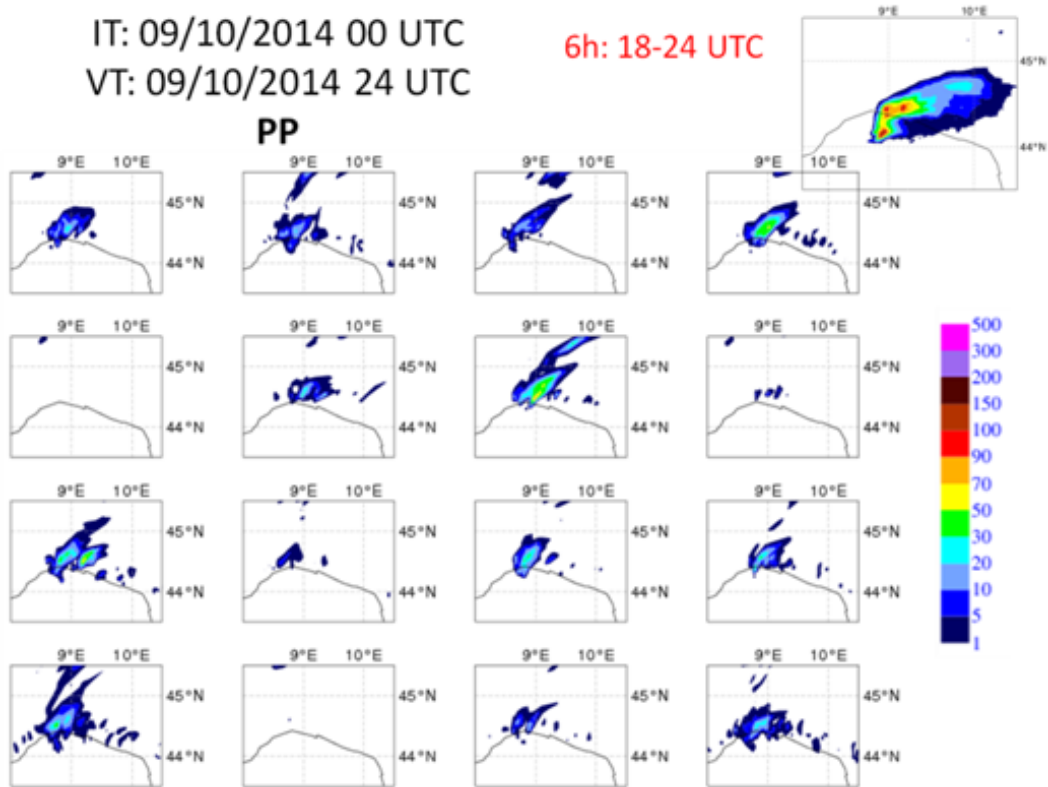


Figure 17: Same as Fig. 16 but for the PP ensemble.

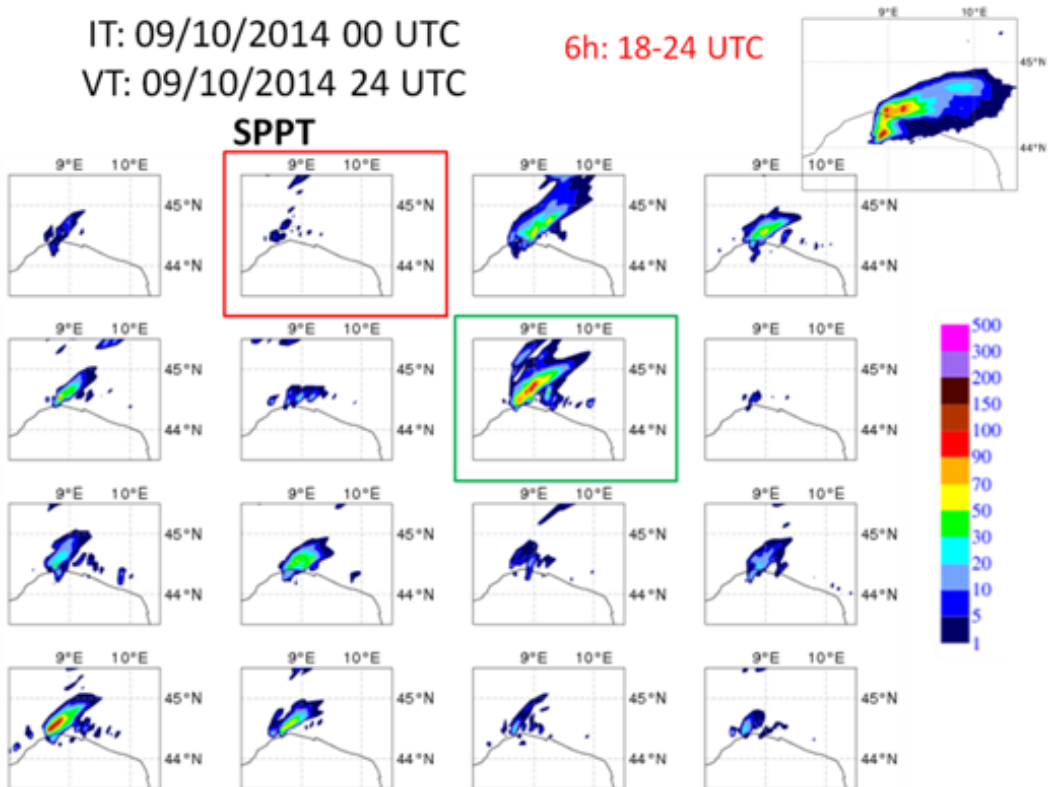


Figure 18: Same as Fig. 16 but for the SPPT ensemble.

The different role of the 2 perturbations in modifying the ensemble forecast for this case

is highlighted by considering the maps of ensemble mean and ensemble spread for the accumulated precipitation (Fig. 19). The PP ensemble (middle panel) forecasts an area of precipitation broader and more extended to the east than the downscaling ensemble (left panel), partly addressing the localisation error highlighted above, while the SPPT (right panel) mainly enhance the precipitation intensity, and adds spread particularly in the area where the precipitation peak was already forecasted by the downscaling ensemble.

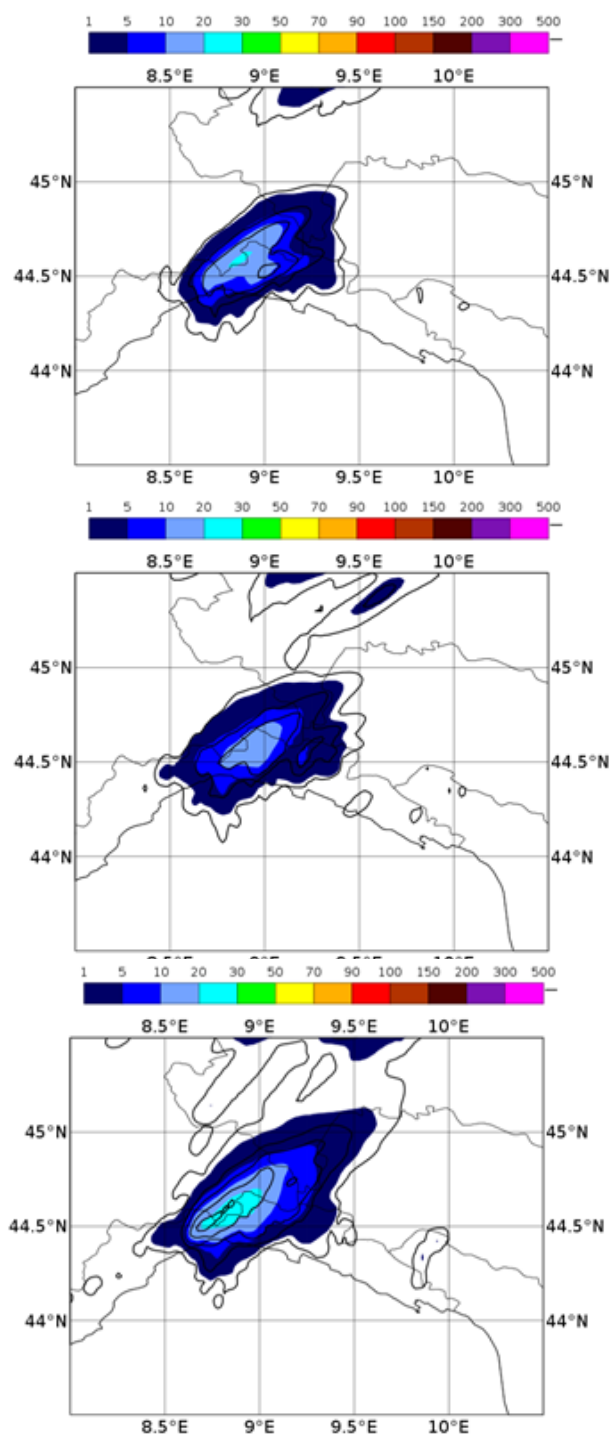


Figure 19: Ensemble mean (shaded) and spread (contouring) of the precipitation forecasted by the downscaling (left panel), PP (middle panel) and SPPT (right panel) ensemble, accumulated over the 6 hours between 18 and 24 UTC of the 9th of October.

Considering the Parma case, the precipitation forecasted over the 24h by 4 selected mem-

bers is shown in Fig. 20, for the downscaling ensemble (left column, labelled no physics perturbation in the Figure) and for the SPPT ensemble (right column). Also from this case is evident that SPPT tends to forecast more intense precipitation but does not address the issue of the localisation of the structures. Conclusions from these runs were drawn, by noticing that for the two cases the 2.8 km ensemble is able to provide scenarios different from the deterministic run, with few good members. The error in the localisation of the rainfall pattern is addressed by some model perturbations, but initial and boundary conditions seem to play a major role. Finally, SPPT-perturbed runs have a tendency towards more intense precipitation.

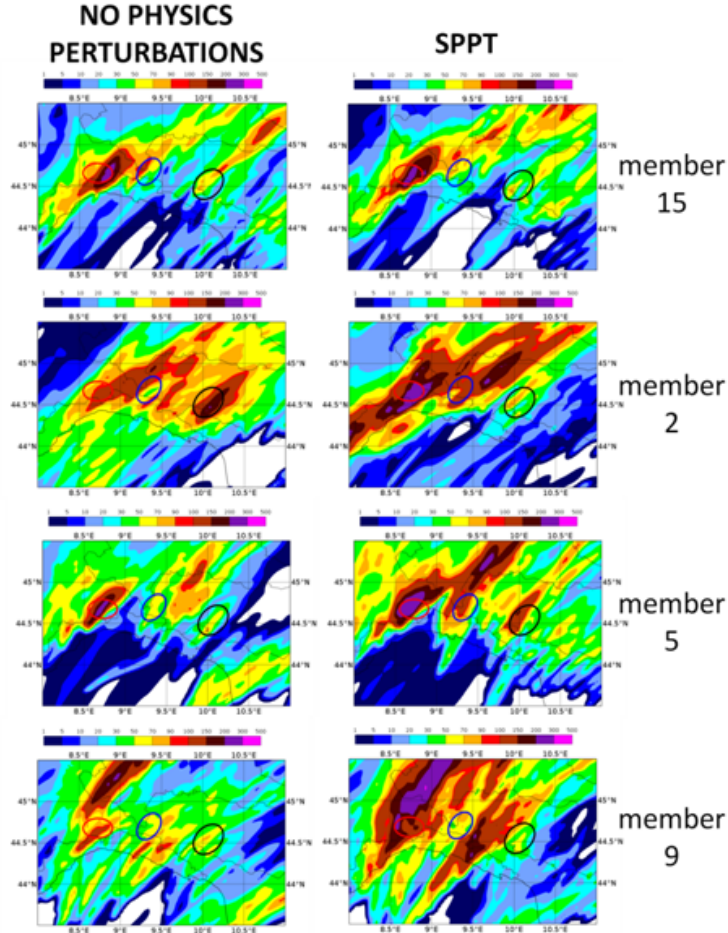


Figure 20: Precipitation forecasted by 4 members of the downscaling (left column) and SPPT (right column) ensembles, accumulated over 24 hours on the the 13th of October.

3.2 Test of the SKEB scheme in the 2.2 km ensemble at MCH

SKEB has not been further tested in COSMO, since the code is far from being ready for operational use due to performance issues. On the other hand, the generated perturbations are similar to those of the random pattern generator developed by RHM which has been implemented in COSMO with no performance problems. Hence, further work in this direction should preferably use this random pattern generator.

3.3 Information about improvements and a new strategy for model perturbations at DWD

At DWD, the research in model perturbations has been focussed on two aspects. On the one hand, the operationally used approach of fixed, non-stochastic perturbations of physics parameters has been extended and methodical modifications have been tested. On the other hand a prototype of a new model perturbation strategy with stochastic components has been developed and tested (model for the model error). The current set-up has been improved by including more parameters in the perturbation set up, i.e. the perturbation of minimum diffusion coefficients for heat and momentum has been added in the operational set-up in January 2014. Moreover, successful tests have been carried out for more perturbed parameters which have been selected with special focus on renewable energy applications. In general, adding more perturbed parameters led to a slight increase in ensemble spread with neutral or slightly positive impact on the root mean squared error of the ensemble mean. As a further methodical modification, which additionally helps to effectively perturb more parameters, a randomized selection of the perturbed values has been developed and first tests have been carried out. While there are still 2 -3 pre-defined different values for the parameters to be perturbed, there is a random approach how these perturbations are distributed within the 20 members. Under the condition that each parameter is perturbed in 50% of the members, a random selection of members which are actually perturbed is done for each parameter at each forecast start time. The selected perturbations stay fixed over the forecast range. Thus, the new method is not stochastic with respect to parameter values but used to distribute pre-defined values effectively among members and the EPS differs in this respect between forecast starts. Again, an increase of spread without degradation of skill (RMSE) has been observed. These refinements of the method became operational in November 2016. The research, which is intended to lead to a new perturbation strategy in upcoming years, is based on the assumption, that the temporal evolution of the model error itself can be described by an equation taking into account temporal and spatial coherence and a white noise stochastic component. The parameters of this model for the model error are estimated from past data and are considered to be weather-dependent. A prototype of this method has been implemented, tested and refined. Considerable resources will be denoted to further research on scientific and technical issues of this new strategy during the next years with the aim of operational implementation. Information on the advances concerning model perturbations has been provided to COSMO at the General Meetings and during the WG7 Meetings.

4 Soil/surface perturbations

The sensitivity of moist atmospheric processes to soil conditions has been demonstrated in numerous studies (Hacker 2010 and references therein). Although the physical representation of soil moisture in land surface schemes is known to have an influence on the quality of atmospheric predictions, the parametrization of the processes of soil moisture physics is not straightforward and the uncertainty in the parameters are little researched (Cloke et al, 2012). Some techniques have been proposed in the recent years: Cloke et al (2012) proposes a simple method, perturbation of 2 soil scheme parameters, in the ECMWF seasonal forecasting system; Sutton et al (2006) studied the impact of using two different soil moisture fields, estimated by 2 different LSM but with the same data and atmospheric forcing, showing that short-term precipitation is sensitive to the soil moisture, especially for a high-resolution run; a non-cycling surface breeding method has been proposed by Wang et al (2010), where short-range surface forecasts driven by perturbed atmospheric forcing are used for generating the

perturbation to surface ICs. A simple method is applied by Hacker (2010), who constructs perturbations of the soil moisture field that represent random, spatial correlated errors, to quantify the response to soil moisture perturbations. He recognises that this method is not suited for reproducing the characteristics of the actual soil moisture uncertainty, which varies locally with the properties of the soil, vegetation and background moisture itself (Hacker, 2010). In order to partly account for soil moisture uncertainty, in the COSMO PP CONSENS a methodology for soil moisture perturbation based on Sutton and Hamill (2004) was developed by HNMS (COSMO Technical Report No. 22). The method was never tested in ensemble mode but it could be revived and tested on the new ensembles under development. Other methods can be tested, among those available in literature, or proposed, according to the need of the COSMO countries and on the available resources. At DWD a simple method was developed to derive initial condition soil moisture perturbations from differences between COSMO-EU und COSMO-DE soil moisture. A long period test is now planned. Within the COTEKINO PP, work on soil/surface perturbation has been carried out at IMWG and at Arpa Piemonte. First a sensitivity study have been carried out, indicating a great sensitivity of COSMO run at 2.8 km to the soil conditions, in particular soil moisture and few TERRA parameters. Secondly, a scientific investigation of the possible strategies to be followed has been performed, including literature review and assessment of the more suitable methods. Then, techniques for lower boundary perturbation have been developed in the two Centres and have been implemented on selected cases. This work is described in detail in the following subsections.

4.1 IMGW

4.1.1 Preliminary sensitivity tests

The first part of this work focused on the test of different set-ups (configurations), in terms of parameters and methods. Shallow convection scheme was chosen as a basic (and invariant) setup to subsequent studies, because of the grid resolution used in the simulations (convection-permitting). As it was described in the previous work (Duniec and Mazur 2014), the other physical parametrizations and numerical schemes selected for the test were as follows (see also Schättler et al. 2016, for details):

- The various formulations of the advection:
 - Leapfrog: 3-timelevel HE-VI (Horizontally Explicit - Vertically Implicit) Integration. This scheme is used as default in Poland for the 7km resolution operational model, as well as for COSMO-EU at DWD
 - Runge - Kutta: 2-timelevel HE-VI Integration (irunge_kutta=1). This scheme is used in COSMO-DE
 - Runge - Kutta: 2-timelevel HE-VI Integration (irunge_kutta=2) - variant scheme with Total Variation Diminishing
- Vertical turbulent diffusion:
 - 1-D diagnostic closure (used in combination with leapfrog scheme only)
 - 1-D TKE-based diagnostic closure (used in COSMO-EU and in COSMO-DE)
- Type of parametrization for transpiration by vegetation:
 - Bucket version

– BATS version

All the above gives a total of 9 basic (reference) set-ups. Then soil-related parameters to be evaluated in the sensitivity test were chosen as follows:

- `c_soil` (with relation to `c_lnd`) - surface-area index of evaporating fraction from 0 to `c_lnd` (surface-area index of gridpoints over land, default 1.0),
- `crsmin` - minimum value of stomatal resistance (used in connection with BATS version only) from 50 to 200 (default 150.0),
- `pat_len` - length scale of subscale surface parameters over land from 0 to 10000 (default 500 m)

all the above are in the TUNING namelist. In addition:

- `cz_bot_w_so` - depth of bottom of last hydrological active soil layer, from 0.0 to last soil level depth (default 2.0 meters), in the PHYCTL namelist.

The general assumption for the preliminary assessment was to choose three to four values from a given parameter range, including minimum and maximum ones. Output fields selected for comparison were:

- Soil - soil temperature at 0 cm down (surface temp.).
- T2m - air temperature at 2m above ground level.
- Water - water + ice content of soil layers 1cm down the surface.
- U10m - zonal wind component, 10m above ground level.
- V10m - meridional wind component, 10m above ground level.

Statistical characteristics selected for the sensitivity analysis are here listed included the standard scores (BIAS, RMSE) as well as other measures here listed:

- the point-to-point difference field with centre of mass of field of differences is defined in Eq. 1 t_x being the value of the field at point r_x , average difference and RMS of difference (over entire domain)
- the maximum difference of values (MDV) defined in Eq. 2 where r and c are reference and changes, respectively
- the normalized difference of values NDV (Eq. 3) with $\langle T_x \rangle$ defined in Eq. 4
- the R (Pearson) correlation coefficient (over entire domain) defined in Eq. 5

$$\vec{r}_d = \frac{\sum_{\vec{r}_x} t_x \cdot \vec{r}_x}{\sum_{\vec{r}_x} t_x} \quad (1)$$

$$MDV = \max[|t_r(i, j) - t_c(i, j)|] \cdot \text{sign}[t_r(i, j) - t_c(i, j)] \quad (2)$$

$$NDV = \frac{\langle T_c \rangle - \langle T_r \rangle}{\langle T_r \rangle} \cdot 100\% \quad (3)$$

$$\langle T_x \rangle = \frac{\sum_{i=1}^{i_{max}} \sum_{j=1}^{j_{max}} t_x(i, j)}{i_{max} \cdot j_{max}} \quad (4)$$

$$R = \frac{\sum_{i=1}^{i_{max}} \sum_{j=1}^{j_{max}} (t_c(i, j) - \langle T_c \rangle) \cdot (t_r(i, j) - \langle T_r \rangle)}{\sqrt{\sum_{i=1}^{i_{max}} \sum_{j=1}^{j_{max}} (t_c(i, j) - \langle T_c \rangle)^2} \sqrt{\sum_{i=1}^{i_{max}} \sum_{j=1}^{j_{max}} (t_r(i, j) - \langle T_r \rangle)^2}} \quad (5)$$

As a case study basis eleven different synoptic situations were chosen (for Poland area); six of them were tested also in the framework of the COLOBOC Priority Project, and five new ones:

- 2009.02.01 (00 UTC) - low temperature, the ground was frozen solid
- 2009.02.22 (12 UTC) - sunny/fair day
- 2009.10.16 (00 UTC, 06 UTC) - ground covered with snow
- 2009.11.04 (12 UTC) - windy day with precipitation
- 2009.11.21 (06 UTC) - foggy day
- 2012.02.03 (00 UTC) - very cold day with air temperature below -20°C, ground frozen solid after two weeks of low air temperatures
- 2012.05.18 (00 UTC) - sunny/fair day, ground temperatures below 0°C
- 2012.07.01 (00 UTC) - sunny/fair/hot day
- 2012.12.14 (12 UTC) - again, very cold day with air temperature below -10°C
- 2012.12.16 (12 UTC) - right after previous, some warming in the air (higher temperature)

As a consequence of the results of these tests, the following conclusions were drawn (Duniec and Mazur, *ibidem*):

- No significant differences (sensitivities) with changes of numerical schemes (HE-VI, RK1 and/or RK2) were observed. Therefore, authors suggested to focus in the subsequent work on the COSMO operational configuration (i.e., 3-order standard Runge-Kutta scheme, 2-timelevel HE-VI integration)
- `cz_bot_w_so` has a noteworthy impact on values of water and ice content down to 1458 cm below ground level
- Parameter `c_soil` has a noteworthy impact on values of air temperature at 2m, dew point temperature and relative humidity at 2m, wind speed and direction at 10m and surface specific humidity
- For the other parameters no significant impact of the tested values against the reference ones was found.

Consequently, extended sensitivity tests were carried out with the following assumptions:

- CP-scale and model resolution forced the use of shallow convection scheme
- 3-order standard Runge-Kutta scheme was selected as a basic numerical scheme
- Different synoptic situations, i.e. the eleven cases listed above, were used to establish a relation between the stochastic variation of $c_{\text{soil}}/cz_{\text{bot_w_so}}$ parameters and the skill of the ensemble members

The following figures (Figs. 21-28) show selected results from the sensitivity tests. Results are described in terms of the spatial distribution of the “spread” - i.e. standard deviation of the ensemble members vs. control (deterministic) run - for the selected parameter and presented as the “spread” (from left to right) of temperature (a), dew point (b), wind speed (c) and precipitation (d).

- c_{soil} sensitivity test results:

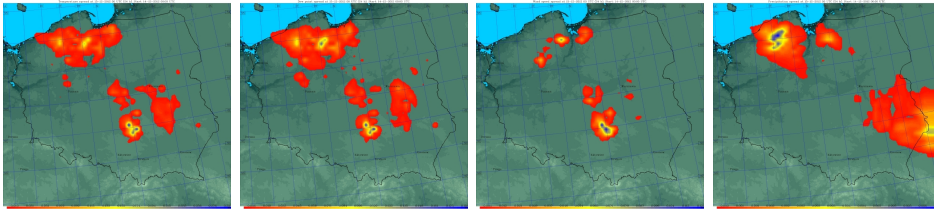


Figure 21: Winter case (December 14th, 2012). a, b, c, d from left to right respectively.

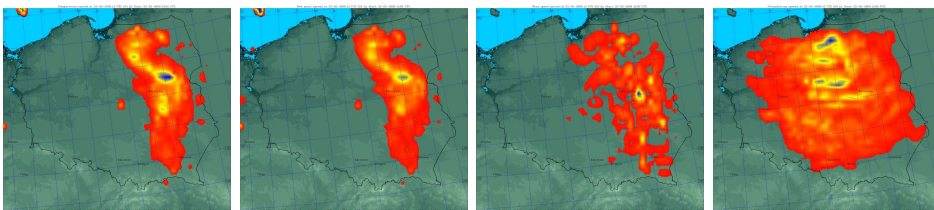


Figure 22: Spring case (February 22nd, 2009). a, b, c, d from left to right respectively.

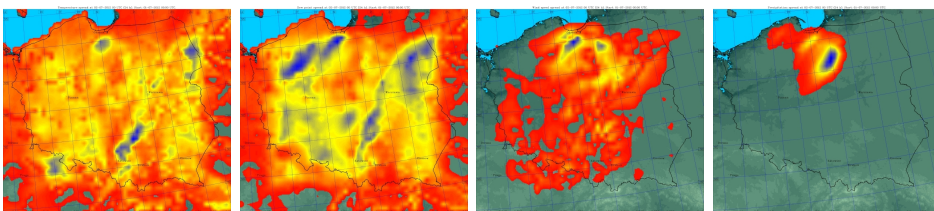


Figure 23: Summer case (July 1st, 2012). a, b, c, d from left to right respectively.

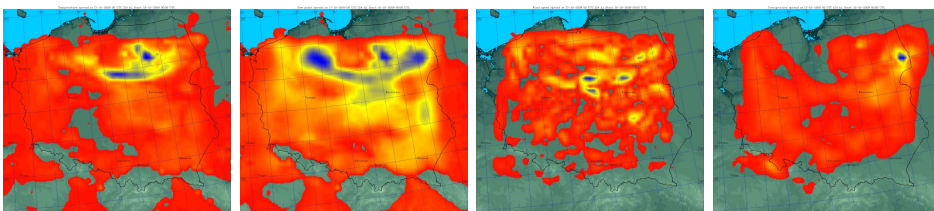


Figure 24: Autumn case (October 16th, 2009). a, b, c, d from left to right respectively.

- cz_bot_w_so sensitivity test results:

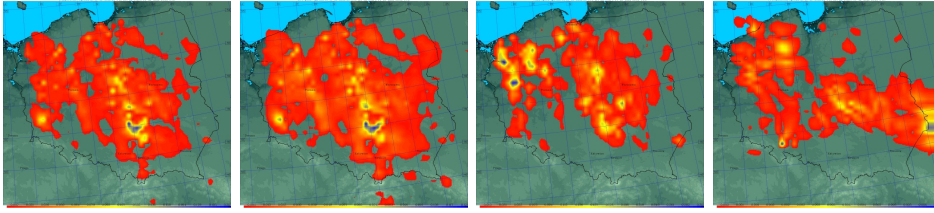


Figure 25: Winter case (December 14th, 2012). a, b, c, d from left to right respectively.

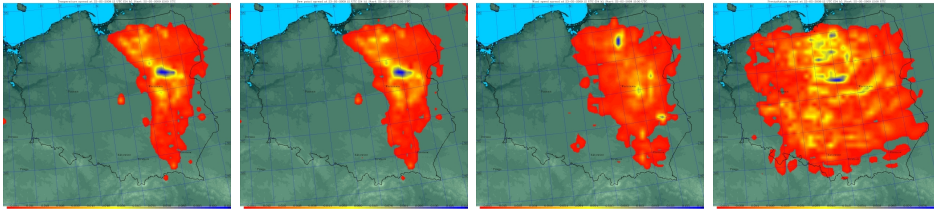


Figure 26: Spring case (February 22nd, 2009). a, b, c, d from left to right respectively.

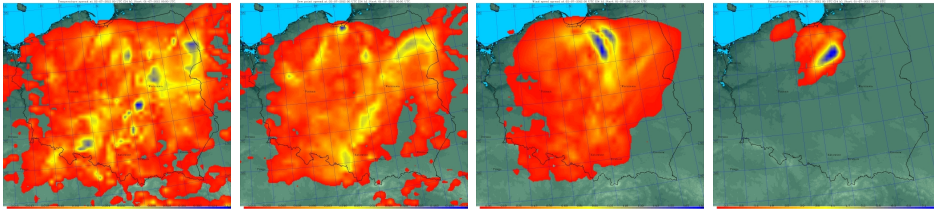


Figure 27: Summer case (July 1st, 2012). a, b, c, d from left to right respectively.

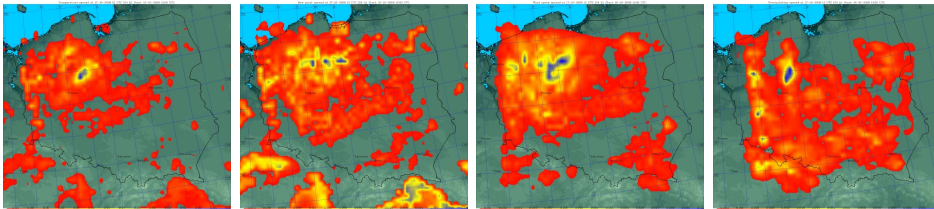


Figure 28: Autumn case (October 16th, 2009). a, b, c, d from left to right respectively.

It should be stressed that changes of cz_bot_w_so had a noteworthy impact on values of “deep soil” parameters, like water/ice and water content, temperature of soil layers down to 1458 cm (not shown). This influence varied from 10 to 25 percent of original (reference) value, and seemed to enlarge with increase of cz_bot_w_so. Impact on values of lower-atmosphere parameters like air temperature, dew point, precipitation amount or wind speed is regarded as negligible. Moreover, this parameter - which is of integer type, from 1 to 7 - seemed to be not very useful for the preparation of an ensemble. On the opposite, changes of c_soil seem to induce significant changes of values of air temperature, dew point temperature and relative humidity at 2m, wind speed/direction at 10m and surface specific humidity forecast against reference ones. Being a floating-point number it may be equal to any value in its range of variability (ie. from 0 to 2.0), so c_soil is (potentially) a much better candidate as a perturbation for an ensemble. Thus, all selected cases were studied in detail regarding changes of c_soil parameter (Mazur and Duniec, 2014a). The maximum “spread” (standard deviation of values against reference one) - is as big as 2°C (for temperature or dew point)

or 1.5 m/s (for wind-speed). Mean difference (over the entire domain) between maximum and minimum values was about 0.1°C and 0.07 m/s, respectively. This order of changes pertained mostly to “warm” cases (late spring, summer, early fall), since the soil is at this time much more “subtle” to “stimuli” from a boundary layer. Thus, all the changes seemed to be much more visible during the warm season as above defined. Impact on values of soil parameters like water/ice and water content, or soil layers temperature is rather irrelevant. In the framework of the COTEKINO Priority Project it was planned to study the possibility to prepare a suitable ensemble in two different ways. The first one was a random setting of the value of `c_soil` globally and uniformly over the entire domain, which is easier to perform with no need for modification of the source code. The second approach proposed was a more “stochastic” one, consisting of a modification of the source code to perturb the values of `c_soil` from gridpoint to gridpoint over the domain in a random way. Subsequent activities were focused to build ensemble(s) in both ways and to compare results of these approaches. Having results of this approach as a first step (see Duniec and Mazur, 2014; Mazur and Duniec, 2014b), in the second phase further sensitivity tests were performed. This allowed for detailed selection of various configurations and for assessing methods of perturbation of important soil parameters.

4.1.2 Extensive test-cases and sensitivity tests

Effective ensemble members could be prepared using two methods:

- Set a unique random value of `c_soil`, globally on the whole domain. Easier to perform, by changing the namelists instead of modifying the model code
- An alternative approach - distribute the random values of the `c_soil` from point to point over the entire model domain by modifying the source code

The results are described in terms of spatial distribution of forecast “spread” - i.e. the standard deviation against mean value. As a case study basis, eleven events were chosen, covering four seasons and a diversity of synoptic situations. In Figs. 29 and 30 results of an application of the above mentioned point-to-point method for preparation of an ensemble, are presented.

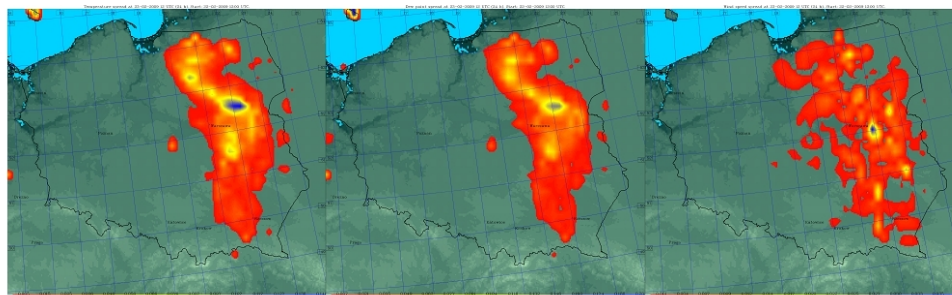


Figure 29: Spread of selected meteorological field from a `c_soil` based ensemble; winter case (February 22nd, 2009). Temperature (left), max spread value - 0.2°C, dew point temperature (middle), max spread value - 0.2°C, wind speed (right), max spread value - 0.1m/s.

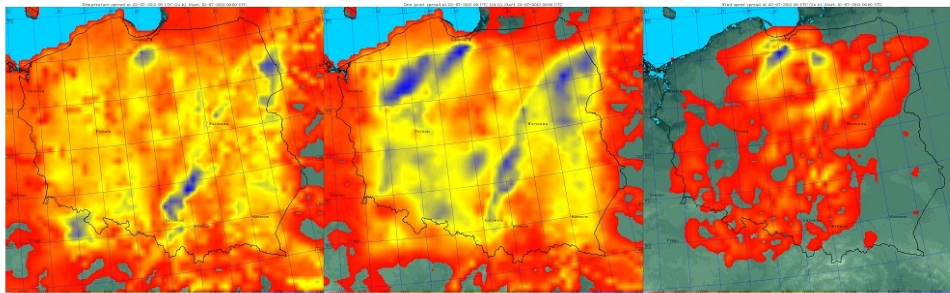


Figure 30: Spread of selected meteorological field over a *c_soil* based ensemble; summer case (July 1st, 2012). Temperature (left), max spread value - 0.7°C, dew point temperature (middle), max spread value - 0.9°C, wind speed (right), max spread value - 1.0m/s.

In Figs. 31-36 results of the comparison of ensemble forecasts with measurements at meteorological stations (seashore station Leba, midland station in Warsaw and Poznan, and the mountain station Zakopane) are shown for selected (winter and summer) cases.

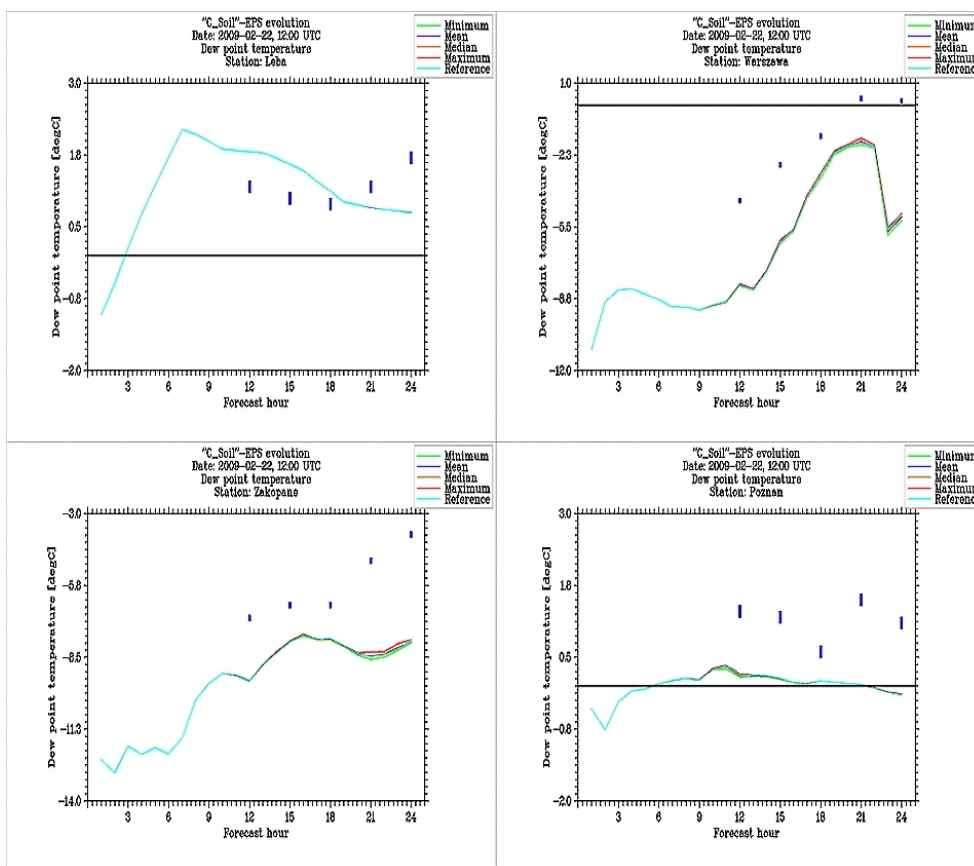


Figure 31: Ensemble forecast with *c_soil*, for the winter case, February 22nd, 2009. “Spaghetti-plots” against values measured at meteorological stations (vertical bars). Dew point temperature forecast at the following stations: upper left - Leba, upper right - Warsaw, lower left - Poznan, lower right - Zakopane.

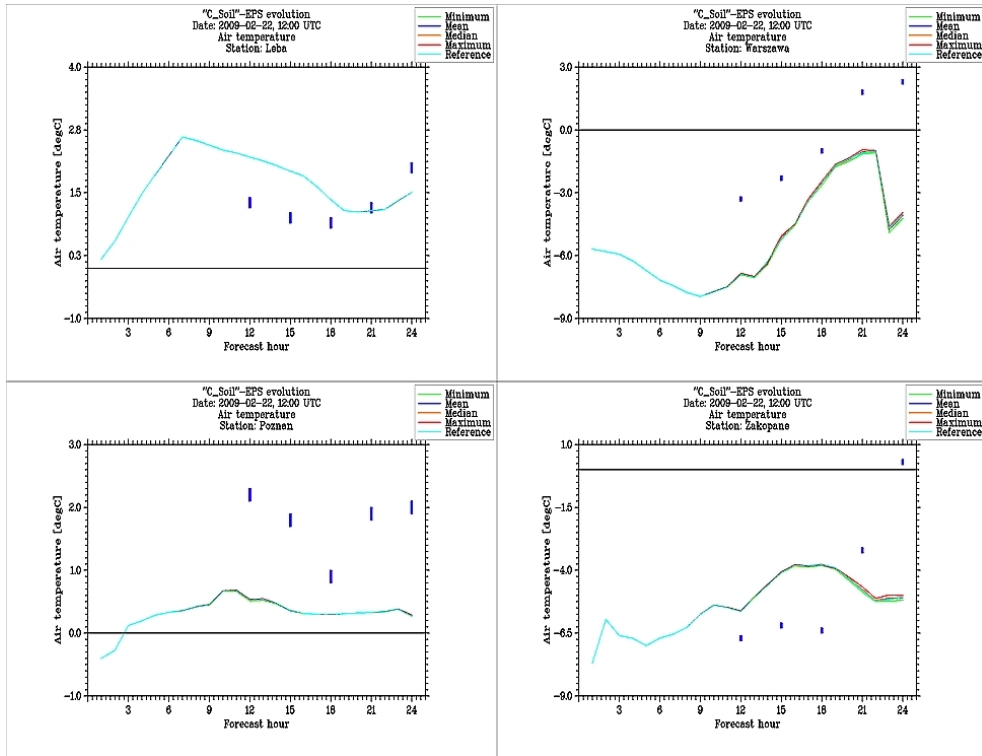


Figure 32: As above, but for air temperature forecast.

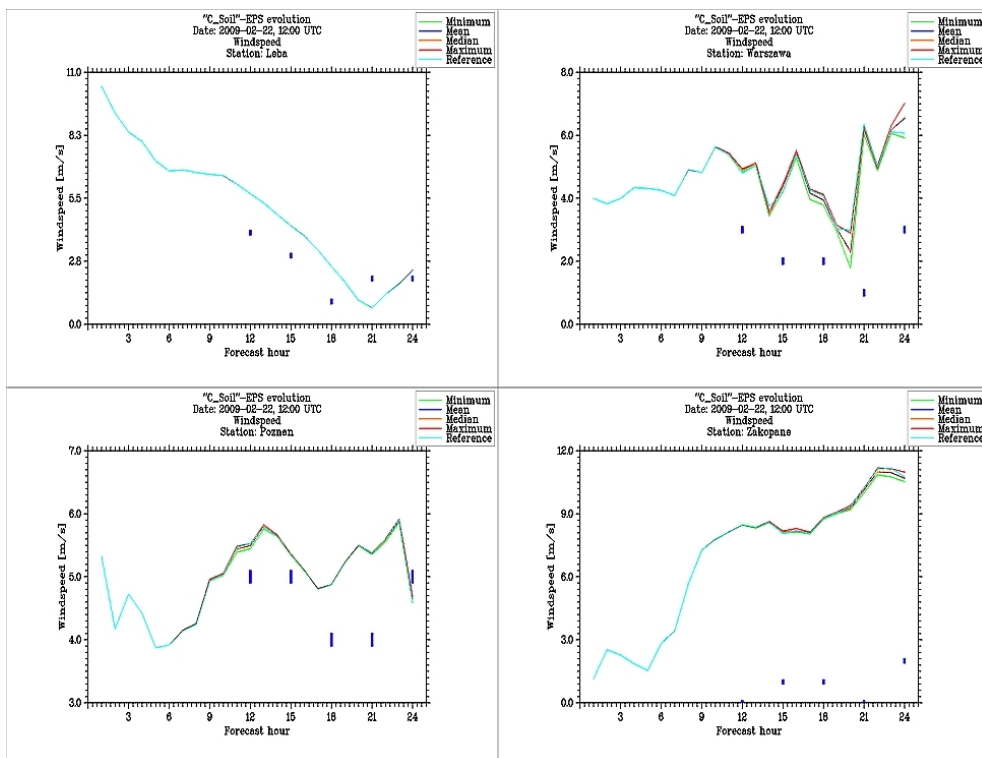


Figure 33: As above, but for wind speed forecast.

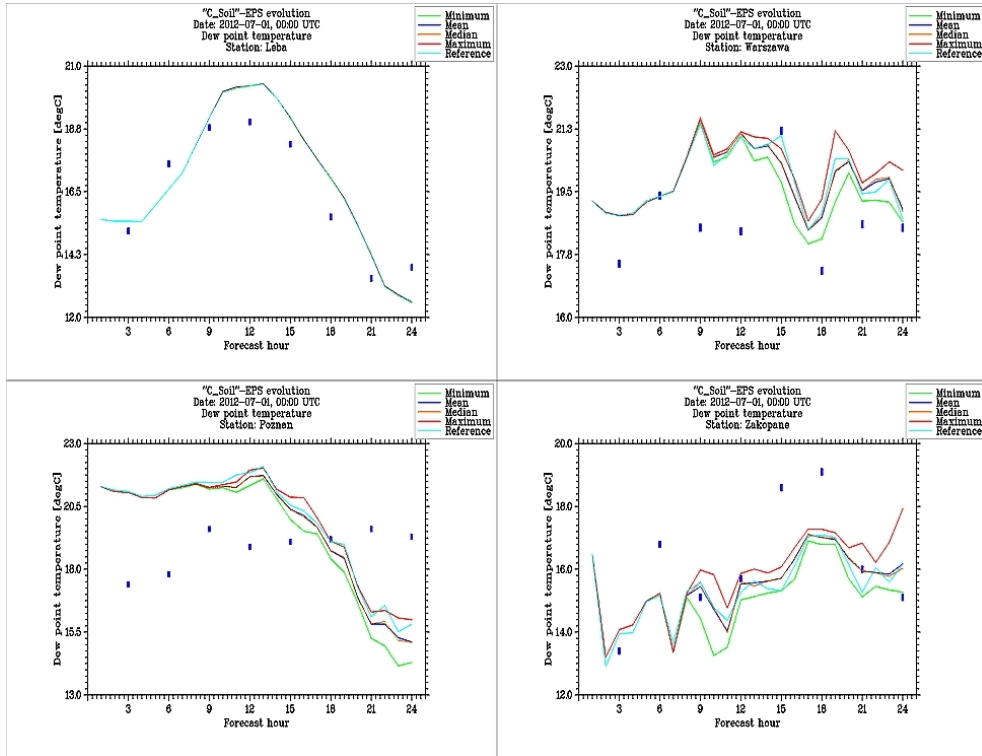


Figure 34: Ensemble forecast with c_soil, summer case, July 1st, 2012. "Spaghetti-plots" against values measured at meteorological stations. Dew point forecast at stations: upper left - Leba, upper right - Warsaw, lower left - Poznan, lower right - Zakopane.

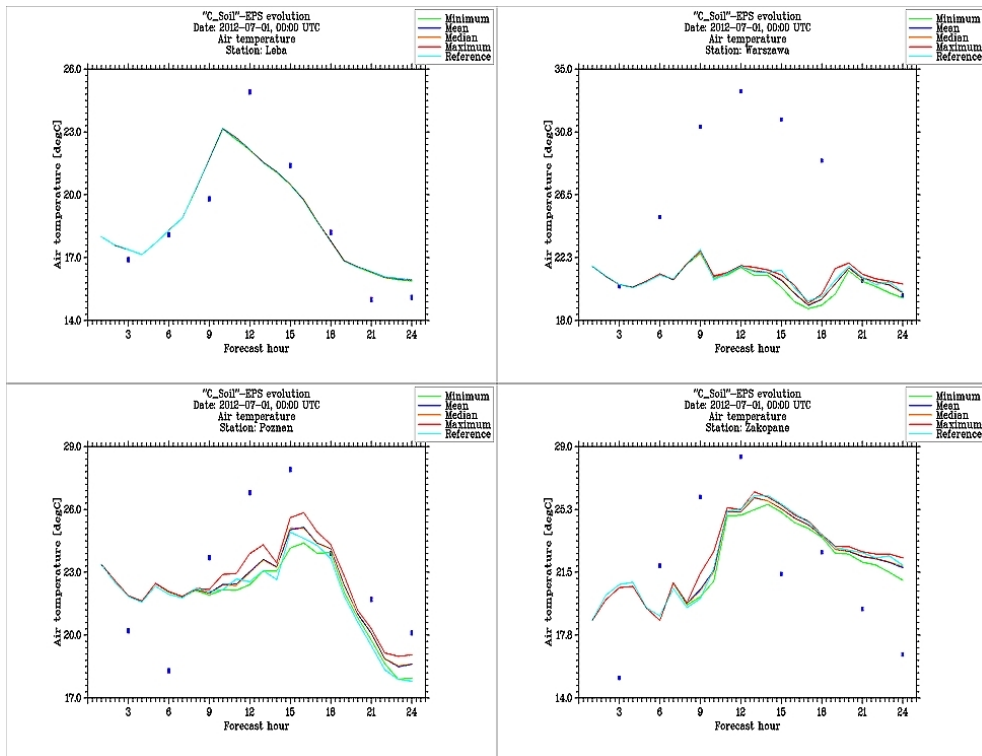


Figure 35: As above, but for air temperature forecast.

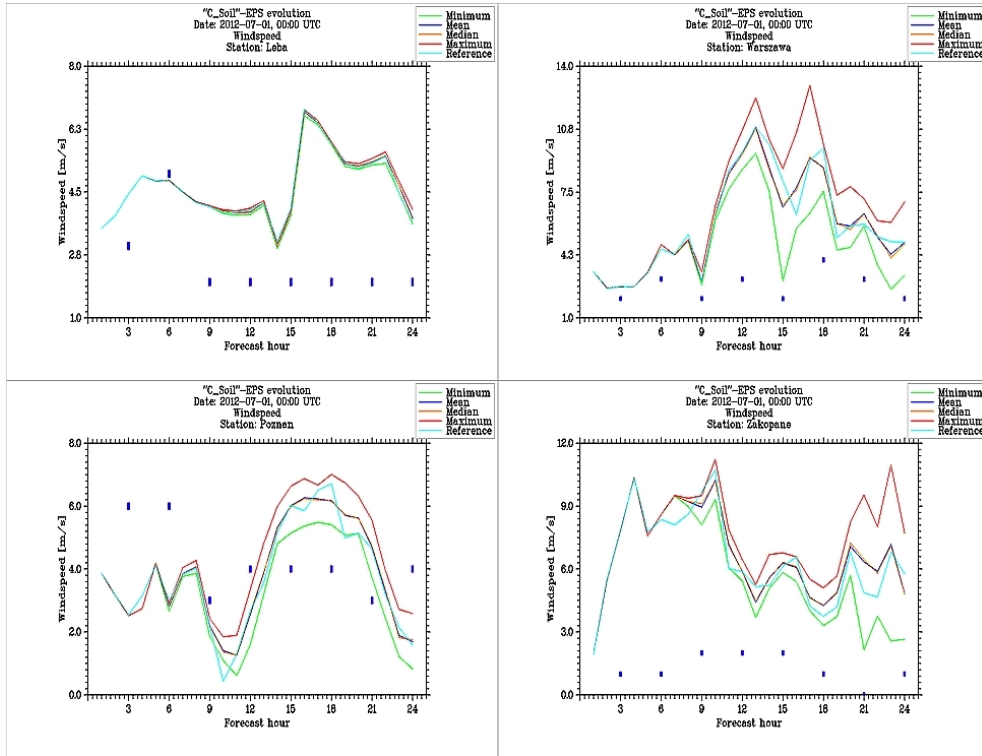


Figure 36: As above, but for wind speed forecast.

The next part of this study was to combine changes in the soil processes parametrization (Duniec and Mazur, 2014, developed by IMGW in the framework of WG3b activities) with the preparation of soil-based ensemble forecasts. After replacing the Dickinson equation with the temperature-dependent Darcy equation (see the above mentioned paper for detailed explanation), further improvements in forecasts can be seen. A quantitative effect of two different soil processes parametrization on a forecast quality was shown in Figs. 37-38. A comparison of these two forecasts was carried out by computation of a “distance” of a real value, measured at SYNOP stations, from an interval defined by the forecast spread, computed as the difference between minimum and maximum values over the ensemble. If the measured value was located inside the interval, this “distance” was identified as equal to zero. In the figures areas with “warm” colours (from yellow to red) represent an improvement of forecast (i.e., decrease of the “distance” of forecast spread from real values) caused by change of parametrization, whereas areas with “cold” colours (from blue to green) - represent a decrease of the forecast accuracy, both measured in [°C] in case of air temperature/dew point temperature, or [m/s] in case of wind speed. An overall improvement, defined by the sum of these “distances” calculated for all SYNOP stations and for every considered element, is presented in the Table 3.

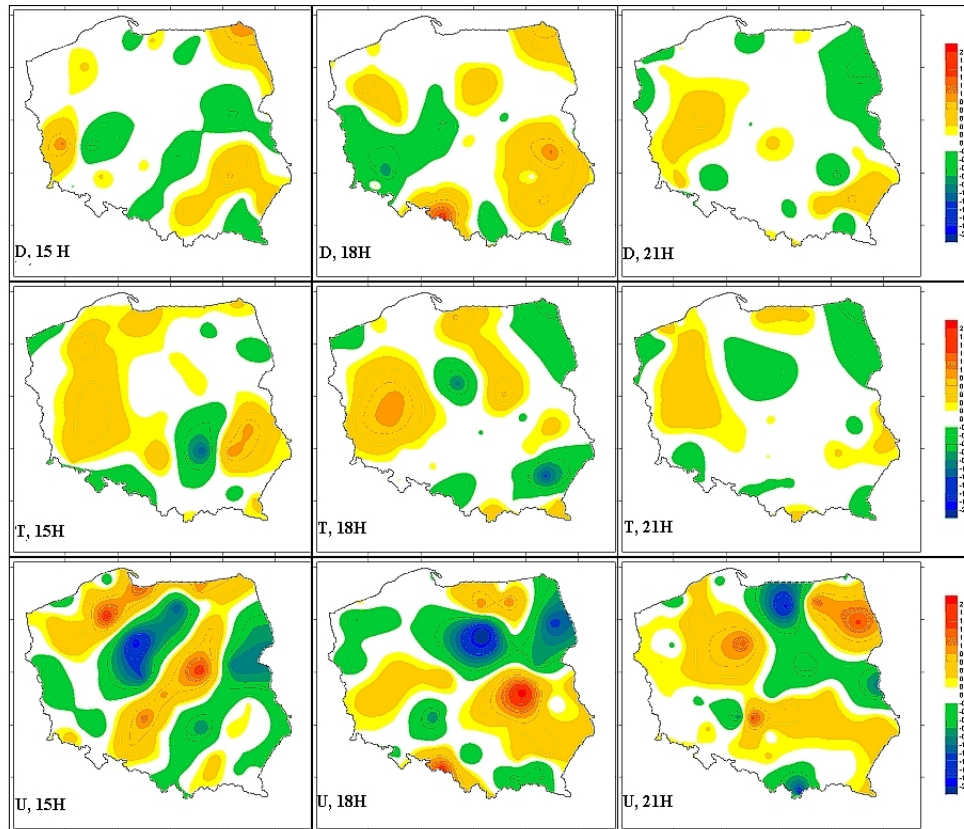


Figure 37: Comparison of “regular” *c*_{soil}-based ensemble forecast with the one combined with altered soil processes parametrization. Summer case, July 1st, 2012. Upper row - prediction of dew point temperature for 15th, 18th, and 21st hour of forecast, middle row - temperature forecast. lower row - wind speed forecast, similarly. Areas with “warm” colours represent improvement of forecast, areas with “cold” colours - worsening of forecast (see further explanation in text) due to change of soil processes parametrization. Scale units: °C in case of air temperature or of dew point temperature, or m/s in case of wind speed, all from -2.0 to 2.0.

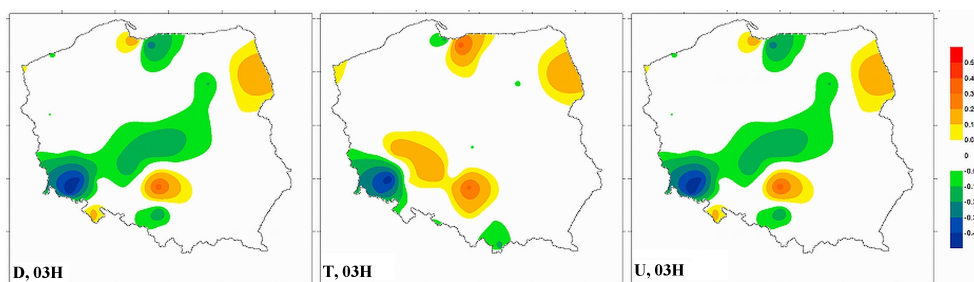


Figure 38: Comparison of “regular” *c*_{soil}-based ensemble forecast with the one combined with altered soil processes parametrization. Summer case, July 1st, 2012. Prediction of dew point temperature, air temperature and wind speed (from left to right) for 3rd hour of forecast. Areas with “warm” colours represent improvement of forecast, areas with “cold” colours - worsening of forecast due to change of soil processes parametrization. Scale units: °C in case of air temperature or of dew point temperature, or m/s in case of wind speed, all from -0.5 to 0.5.

It should also be stated, however, that this improvement can hardly be seen in the beginning of the forecast(s). It seems that the soil parametrization need some “spin-up” time to have a significant impact on the quality of an ensemble forecast of the atmospheric state.

hour of forecast	dew point (°C)	air temperature (°C)	wind speed (m/s)
3	-0.152	-0.071	-0.150
6	0.036	0.149	-0.201
9	-0.013	-0.181	0.143
12	-0.168	0.154	-0.115
15	1.714	4.205	2.016
18	4.701	2.460	1.720
21	1.103	1.969	2.751

Table 3: Indicator of overall improvement/worsening due to combination of ensemble preparations with changes of soil processes parametrization (for details see explanations in text).

In case of dew point and air temperature, significant improvement can be especially seen in the western, north-western and south-eastern part of Poland. In case of wind speed forecasts, the “area of improvement” was moving with forecast hour, in general, from west to east. This could be related to distribution of soil types (mainly areas with sand and loam) in Poland as adopted in the COSMO model (see Doms et al., 2011). Tests proved that small perturbations of selected parameter(s) were sufficient to induce significant changes in the forecast of the state of the atmosphere and to provide valid members in the ensemble. However, perturbations have had almost negligible impact in the areas with land fraction much less than one and during the cold season (perhaps due to the specific soil conditions, e.g. frozen ground). A detailed (seasonal/annual) performance analysis is needed for stochastic forecasts. Comparison of ensemble forecasts with observations at meteorological stations showed that, as in the case of deterministic forecasts, introduction of altered soil processes parametrization slightly improved the forecasts, mainly in the central/southern part of Poland, rather than closer to the sea or in mountain regions. All the results obtained from the tests allow to set-up an operationally running EPS at IMGW.

4.1.3 Test-bed and configuration for (quasi-)operational EPS, concept of time-lagged ICs/BCs

The first approach followed to establish an operational configuration has been carried out with BCs/ICs from COSMO-LEPS. Results were satisfactory from the point of view of the quality (i.e. skill) of the forecasts vs observations, however, time needed to prepare an operational forecast turned out to be unacceptably long, taking into account the downloading and pre-processing of BCs/ICs for the needs of EPS at IMGW. Thus, the idea of time-lagged initial and boundary conditions woke up. An explanation of the concept is presented below. At IMGW-NRI, the COSMO model runs in a deterministic mode using initial (IC) and boundary (BC) conditions from the ICON global model (previously from GME), as shown in Fig. 39. The non-hydrostatic ICON model runs at DWD using an icosahedral-hexagonal grid, with the highest spatial resolution over Europe equal to 13 km and a time span of at least 78 hours, four times per day. The ICON generates a set of IC/BCs for COSMO mesoscale model runs with a basic spatial resolution of 7 km and the domain covering the central part of Europe. This generates 78-hour forecasts. The COSMO model with 7 km horizontal resolution (COSMO-7 km) applies nudging-based data assimilation to correct global model forecasts, ingesting the most recent set of meteorological data acquired from the GTS/WMO network. Forecast results from the COSMO-7 km are further used as IC/BCs for a nested instance of a COSMO model with a higher resolution of 2.8 km and 36-hour forecasts. A set of the deterministic COSMO-2.8 km forecasts define the basis for the operational configuration

Model	Resolution min. (km)	Grid size (NxMxL)	Forecast length (h)
ICON (DWD, former: GME)	13	2949120 triangles	78
COSMO v5.01	7	415x460x40	36
COSMO v5.01	2.8	380x405x50	36

Table 4: Details of the configuration of deterministic models, status for year 2017.

of an ensemble forecasting system. More details of the configuration of deterministic models that run operationally at IMGW-NRI are presented in Table 4.

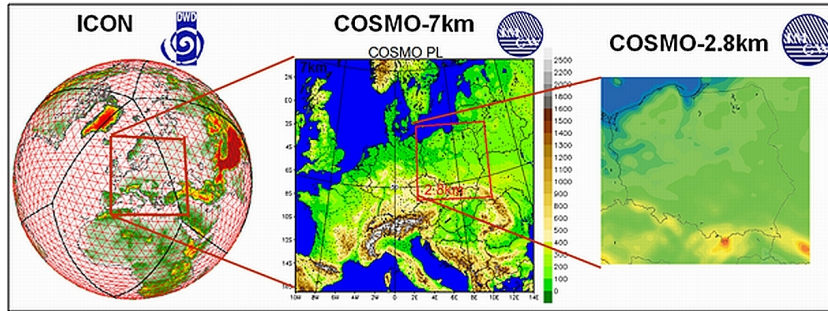


Figure 39: Operational configuration of deterministic COSMO-7 km model and 2.8 km resolution EPS runs at IMGW-NRI. From left to right - domain of ICON global model, domain of COSMO-7 km model running at IMGW-NRI, and a set of nested COSMO-2.8 km domains, forming a 20-members EPS.

In the recently developed EPS configuration, twenty ensemble members are run, based on the COSMO-2.8 km convection permitting (CP) forecasts. Every member of the ensemble applies perturbed lower boundary conditions, composed of a random noise of a specified amplitude added to perturbation of a parameter of the soil-model physical parametrization. The proper collection of adequate initial and boundary conditions (IC/BC) is a crucial issue. In the basic EPS configuration, the whole set of IC/BC was obtained from a single 78-hour deterministic run of the COSMO model with spatial resolution of 7 km. In order to increase the spread of the forecasts, we have further adopted the concept of time-lagged IC/BCs (see e.g. Lu et al., 2007; Chen et al., 2013), in which the set of deterministic CP forecasts is subdivided into groups starting at consecutive time windows: 00, 06, 12, and 18 UTC.

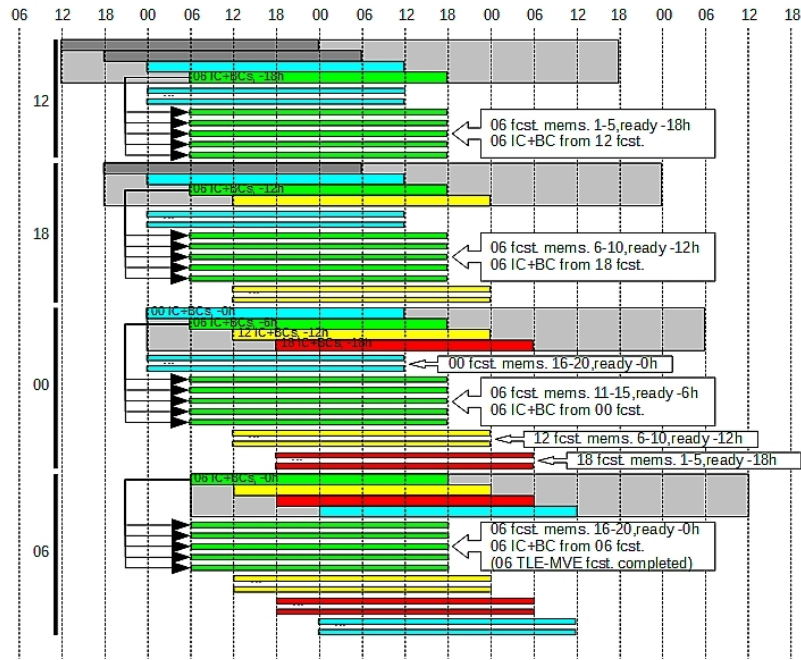


Figure 40: Operational setup of EPS based on Time-Lagged IC/BCs. X-axis - lead time (UTC), Y-axis - forecast individual initial time. The four different colours distinguish forecast nominal start time: blue - 00 UTC, green 06 UTC, yellow 12 UTC, and red 18 UTC.

In the final EPS configuration run operationally at IMGW-NRI, a set of twenty ensemble members is grouped into four bundles, each containing five elements as shown in Fig. 40. The uppermost group - members no. 01 to 05 - is finalized and ready for post-processing 18 hours before the nominal EPS start-up time in the current time window; the second group - members no. 06 to 10 - are gathered 12 hours before the current time window; the third group - members no. 11 to 15 - are prepared 6 hours before the current time window; and finally the lowermost group - members no. 16 to 20 - starts and is finalized in the current time window, completing the whole EPS forecast. The available forecast results (i.e., various meteorological fields) are ready for post-processing in order to provide selected statistics (ensemble mean, ensemble spread, probability of exceedance etc.) in graphical form, suitable for forecasting applications.

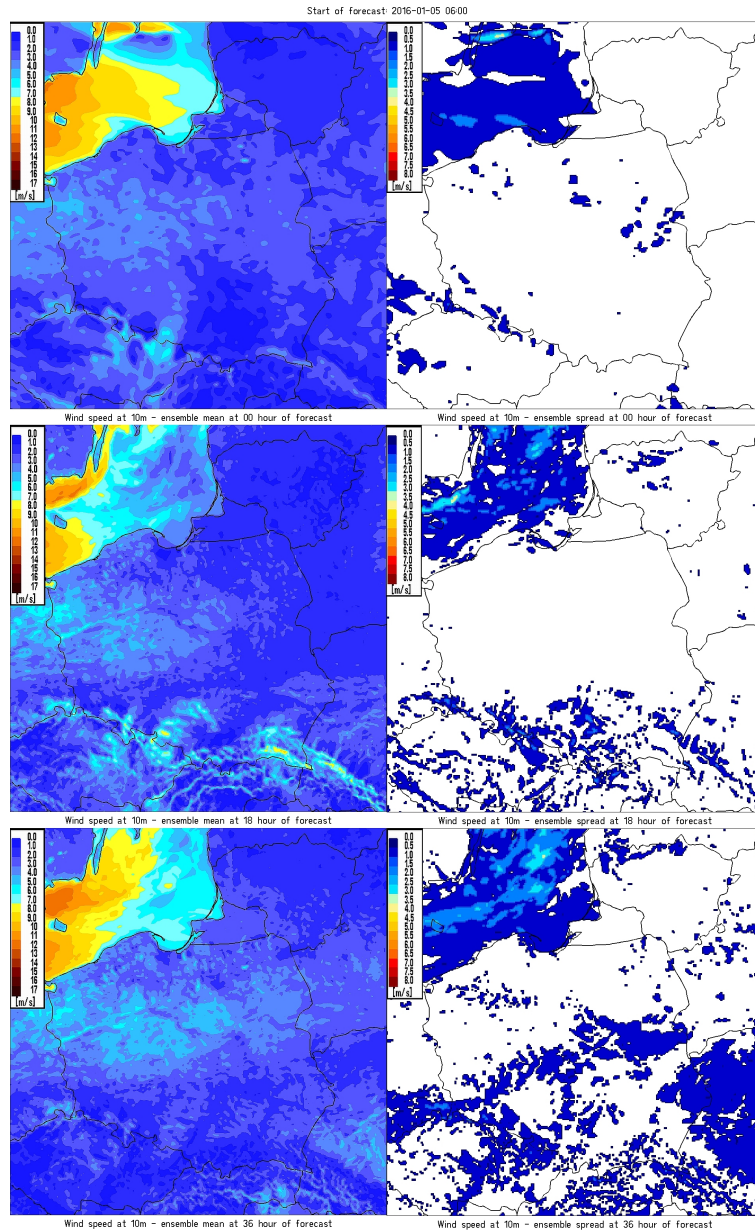


Figure 41: Ensemble mean (left) and ensemble spread (right) of wind speed at 10 m above ground level (m/s) at start (top), at 18th hour (middle) and at 36th hour (bottom) of forecast.

The EPS provides an estimate of the most probable and of alternative realisations of the event. The first two charts in Fig. 41 demonstrate examples of the ensemble mean and ensemble spread of selected meteorological fields (i.e., wind speed at 10 m above ground level). While ensemble spread has the general tendency for underestimation, it helps to objectively estimate the uncertainty of generated forecasts. The low values of the spread mean that forecasts converge toward a similar solution, leading to stronger anomalies. If the spread is large, the atmosphere is in a state where the small changes in the initial conditions may have a large effect on the forecast quality. In Fig. 42 an example of the probability of the exceedance of a selected threshold in the meteorological field is presented. This option is especially useful for calculating the probability of a predefined amount of precipitation (here: 1.5mm/3hours).

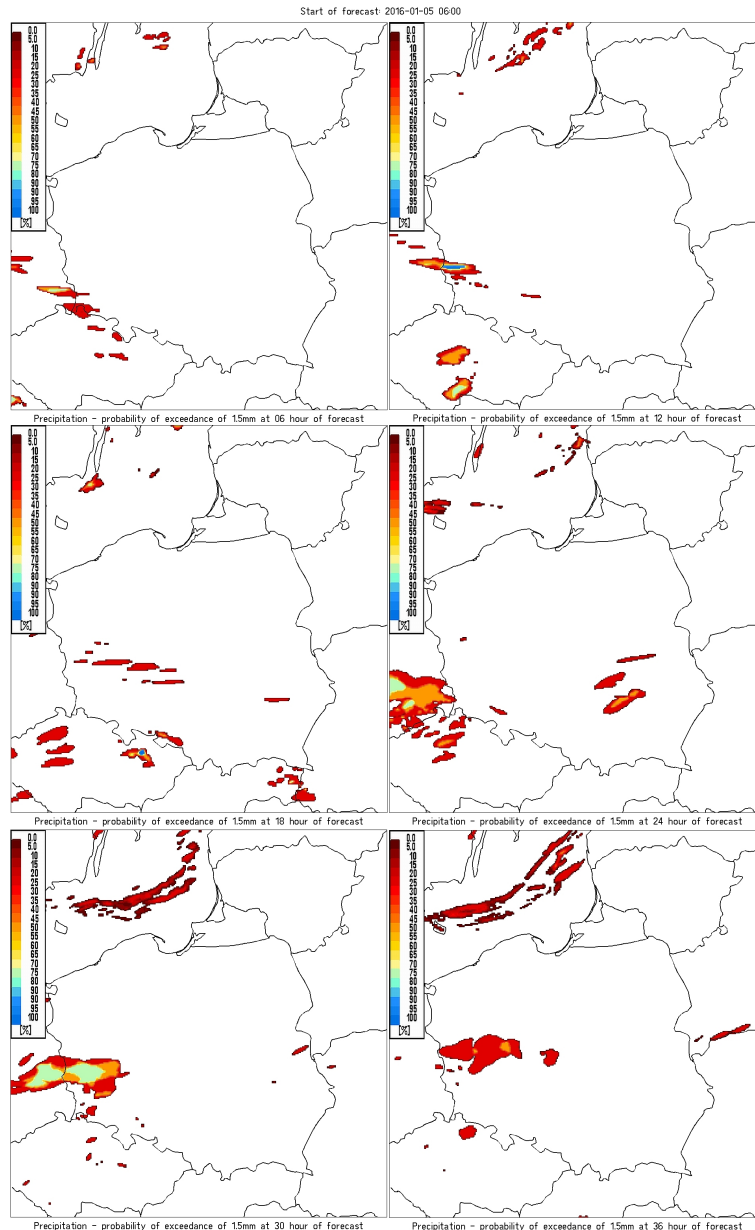


Figure 42: Probability (percentage) of exceedance of precipitation intensity of 1.5mm/3hours at 6th hour (top left), at 12th hour (top right), at 18th hour (mid. left), at 24th hour (mid. right), at 30th hour (bottom left) and at 36th hour (bottom right) of forecast.

In Fig. 43 an example of the so-called “spaghetti plots” is shown - the representation of a selected isopleth of a chosen meteorological field (here, the temperature at 2m above the ground) for every member in an ensemble. Since ensemble members generally diverge in time, these plots show many different model outputs. In the areas where the isopleth pattern is chaotic (i.e., resembling spaghetti) the confidence of the forecast is low. Spaghetti plots provide high confidence of a forecast in regions where members tend to coincide (i.e., contours follow a recognisable pattern through the sequence), and allows for identifying possible clustering of lines (e.g., bi-modal distributions). This particular chart shows an example of the amount of uncertainty in the forecast of air temperature. If there is a good agreement and the contours are close to one another (like in the presented case), then the confidence in the forecast can be high. The presented analysis (as the spread and other probabilistic statistics) derived from ensemble forecasts leads to an increase of confidence

in the forecast and may provide critical information that increases the awareness of a high impact event in advance.

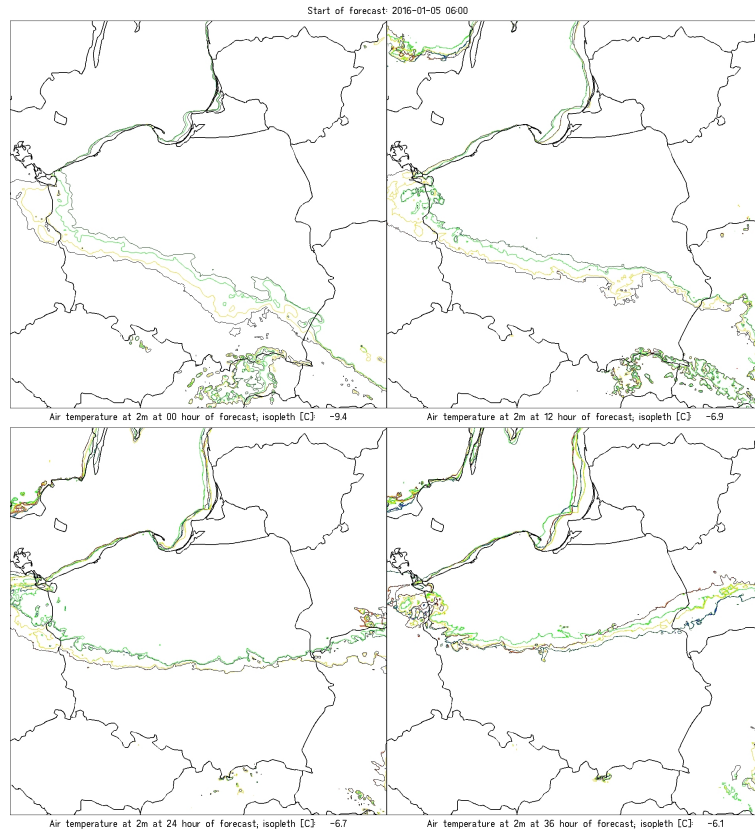


Figure 43: “Spaghetti plots” of air temperature ($^{\circ}\text{C}$) at 2 m above ground level at the start (top left; isopleths -9.4°C), at the 12th hour (top right; -6.9°C), at the 18th hour (bottom left, -6.7°C) and at the 36th hour (bottom right; -6.1°C) of the forecast. Every coloured line represents the spatial distribution of isopleths for a single ensemble member.

The EPS results were compared with observations collected from 61 Polish SYNOP stations. In the following charts (Figs. 44-45) analysis of the model generated air temperature/dew point temperature forecast averaged for the whole day of 5-01-2016 are presented. In both cases, the EPS mean reproduces the main spatial features of the large-scale temperature distribution. The observed temperature is in a similar range (-20.7°C , -2.5°C) to the computed EPS mean (-20.8°C , -3.8°C).

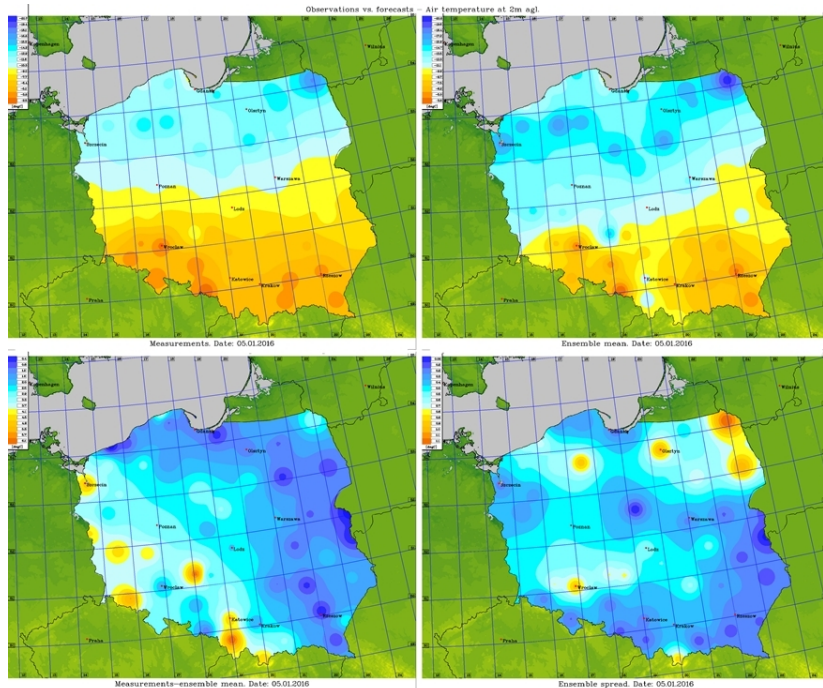


Figure 44: Comparison of the EPS derived temperature: ensemble mean (upper right), spread (lower right) with measurements (upper left), the absolute value of difference between measurement and ensemble mean (lower left).

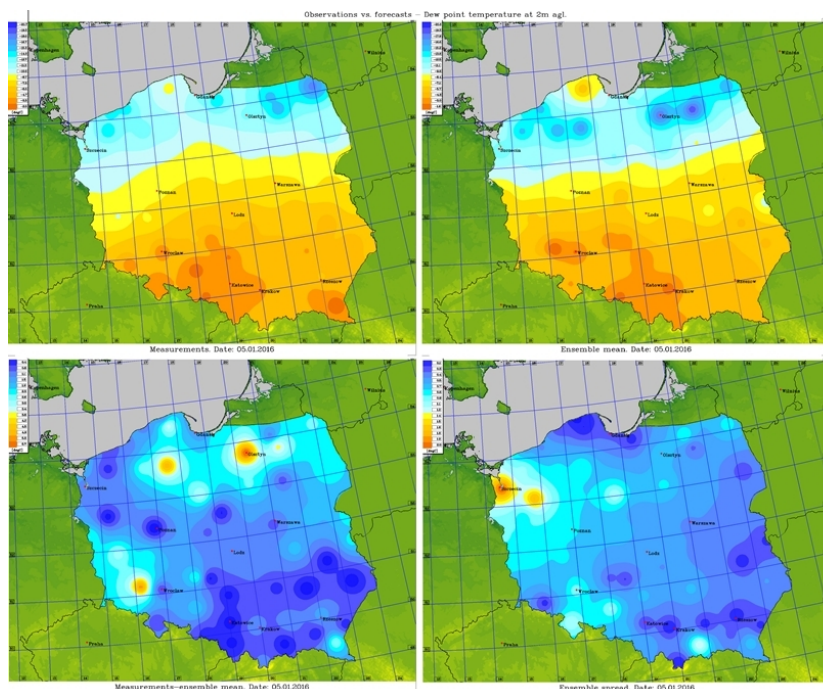


Figure 45: Same as Fig. 44 but for dew point temperature.

Similarly, the observed dew point temperature (Fig. 45) is in a similar range (-20.7°C , -2.0°C) than the EPS computed mean (-20.6°C , -1.6°C). In both cases, the model shows a bias when compared to observations with an absolute error of up to -6.1°C for temperature and -5.7°C for dew point temperature. For the temperature, larger error values (above 3°C) are well correlated with the air masses that came after the warm front crossing Poland during 5

January, 2016. Dew point temperature generally shows a small error - below 2°C- except in the north-eastern part of Poland, where we can observe a persistent lack of cloud coverage and in south-western areas, which may be correlated to a larger exceedance of precipitation intensity (see Fig. 42) that started in the afternoon hours of 5-01-2016 and developed further during the night and the morning hours of the following day. In summary, it should be stated, that our extensive tests conducted during the COTEKINO Priority Project proved that small perturbations of selected soil parameters were sufficient to induce significant changes in the forecast of the state of the atmosphere and to provide valid members to the ensemble (Duniec and Mazur, 2014; Mazur and Duniec, 2014a). Changes of c.soil had a significant impact on values of air temperature, dew point temperature and relative humidity at 2m, wind speed/direction at 10m, and surface specific humidity (ibidem, see also Mazur and Duniec, 2015). The use of the concept of time-lagged initial and boundary conditions allowed us to obtain a valid ensemble and use it efficiently in an operational mode. Further work is intended to focus on “tuning” ensemble performance and to provide quantitative quality scores. For this purpose, a random number generator combined with perturbations of initial soil surface temperature and the dependence of the amplitude of perturbation on soil type will be implemented in the COSMO model. While the set of equally weighted time-lagged forecasts improves short-range forecasts, further progress may also be sought by adopting a regression approach to compute a set of weights for different time-lagged ensemble members. In this approach, the perturbation of the evaporating fraction in the soil has a significant impact on the forecast due to the increased stimulation of energy exchange between the surface and atmosphere. The maximum spread for the temperature is most likely of about 1.1°C, with increased value covering the entire northern and western parts of Poland. For the dew point temperature, we observe a higher spread of the amplitude up to 2.0°C, localized only in the north-western corner of the country. More advanced analysis of the EPS scores and of the correlation between EPS error and spread will be further provided in the context of specific applications. The examples of the probability of the occurrence of dry spells or of rainfall occurrence and distribution are both important in agriculture in assessing the influence of EPS forecasts on irrigation, crop growth or drought occurrence. For synoptic forecasters, the risk of the likelihood of a phenomena and its potential impact will have to be properly estimated to provide the objective basis for a decision to issue a warning. Overall, this phase of project task was focused on:

1. initiatory, quasi-operational implementation of EPS (BCs/ICs from a deterministic 7km runs of COSMO-PL)
2. Post-processing of results general charts/maps of mean/spread/max-min difference, spaghetti-charts of selected meteo elements
3. concept of time-lagged BCs/ICs - idea, technical aspects, details
4. time-lagged BCs/ICs - extended tests of the setup, case study results, quasi-operational implementation.

The work done in the framework of point 1 (and tests with ICs/BCs from COSMO-LEPS) has been presented at the COSMO User Seminars 2015. Further activities, related to points 2-3 have been presented at the COSMO General Meeting 2015, with particular emphasis on the comparison of the results of point 1 with those of points 3 and 4. A contribution has been also published in the COSMO Newsletters No. 14 and 15 as well as in the MHWMM (Duniec and Mazur, 2014; Mazur and Duniec, 2015; Duniec et al., 2017).

4.2 ARPA Piemonte

The goal of this Task was to implement a soil perturbation technique in a high resolution ensemble system based on the Italian version of the limited area model COSMO at a resolution of 2.8 km taking into account soil surface uncertainties. To do this, we performed first a sensitivity test to assess the behaviour of the COSMO model to different lower boundary initial conditions. In fact, even if the sensitivity of the atmospheric moist processes to different soil condition initializations has been demonstrated in several studies, it cannot be generalized to a completely different modelling system. After that, we tried to find the best setting of a soil perturbation technique to be implemented in a high resolution ensemble system based on the Italian version of the limited area model COSMO at a resolution of 2.8 km taking into account soil surface uncertainties.

4.2.1 Sensitivity of COSMO model to different lower boundary initial conditions.

Different models with different spatial resolutions have been chosen to ensure a good variability among the soil moisture fields used to initialize COSMO model for the sensitivity test. A good variability in the ICs of soil moisture fields increases the chance to obtain a good spread among the ensemble members. The sensitivity test has been performed considering case studies taking into account summer and winter conditions, in order to evaluate the potential differences in sensitivity of the COSMO model in different seasons. For the model runs, COSMO model version 5.0 was used, with a horizontal resolution of 0.025 degrees (about 2.8 km), driven by ECMWF reanalysis at 0.125 degrees. The domain of integration is centered on Italy, with 45 vertical levels, 14 of which below 850 hPa. The variables that we opted to analyze for each case study to assess the changing spread due to different initializations were: 2 meters temperature and dew point, 10 meters wind speed (module), vertical velocity (w) at an altitude of about 1000 m, total precipitation, cloud cover, soil temperature and moisture. The spatial average of the spread for all the atmospheric and soil variables considered (Fig. 46), reveals a considerable spread increase for summer (red line), spring (orange line) and autumn (green line) cases, whereas in the winter one (blue line) the increase is less appreciable. Moreover, the diurnal cycle of some variables is evident (temperature, wind speed, and cloudiness), more pronounced in summer and spring conditions and almost absent in the winter stable case. The summer case, showing the highest values in spread and the most pronounced diurnal cycle, is also the one with the lowest initial mean spread. These results can be justified by the fact that during spring and summer seasons the fluxes, namely the exchanges of moisture and energy between soil and atmosphere, are stronger compared to autumn or winter conditions, especially during daytime. For this mechanism, variations in soil moisture may deeply affect the boundary layer and influence atmospheric processes leading to a considerable variability among COSMO runs.

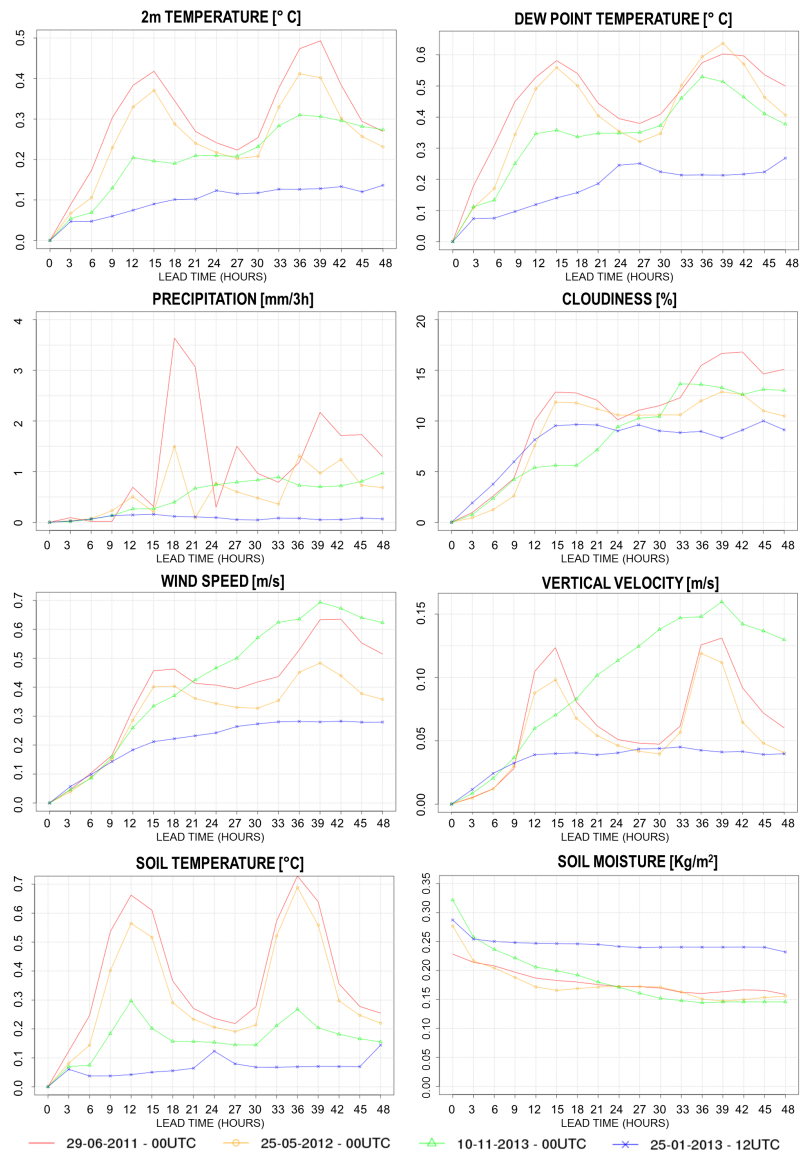


Figure 46: Spread of the variables indicated in panels averaged over the domain as a function of lead time.

This assumption is also confirmed by the behaviour of the soil moisture spread of the first soil layer (bottom right panel). For the winter stable case study, soil moisture spread remains nearly constant, because of the small fluxes leading to a limited exchange of moisture between soil and atmosphere. In other cases, where the fluxes are stronger, the initial spread in soil moisture tends to decrease, especially in the first day of the run. As regard the precipitation spread (left column, second row), the highest values are reached in summer case study with strong synoptic forcing, when events of heavy rainfall occurred. In general, for this variable and for all cases considered, a diurnal cycle is less evident or absent. In fact, for the two convective cases (spring and summer, respectively orange and red lines), thunderstorm events also occurred in the late evening and in the night time, where the cold front or an upper level trough interested some regions of the domain. Hence, in these convective cases, the highest spread generation occurs concurrently with convective phenomena. On the contrary, in the autumn case (green line), less convective precipitation leads to a more uniform spread increase. For the winter case (blue line), no spread appears because of stable synoptic

conditions. Moreover, the soil moisture spread remains nearly constant during the run, as already noticed. To explain this results we have to consider first that a strong inversion layer inhibits the moisture and heat transfer between soil and atmosphere and hence the variability from soil to the surface variable. Second, if the lower boundary layer is already close to the saturation, variations in the soil moisture content probably have a weak effect in the fog formation at the surface. These two points could explain why the influence of soil moisture perturbation in the surface variable is weak for winter case studies. As regard the wind speed and the vertical velocity (third row), the different behavior in spread between spring and summer case studies and the autumn one can be noticed. Considering the convective case studies analysed and as far as precipitation is concerned, we noticed that the areas of large spread are approximately also the regions where the convective phenomena took place (Fig. 47).

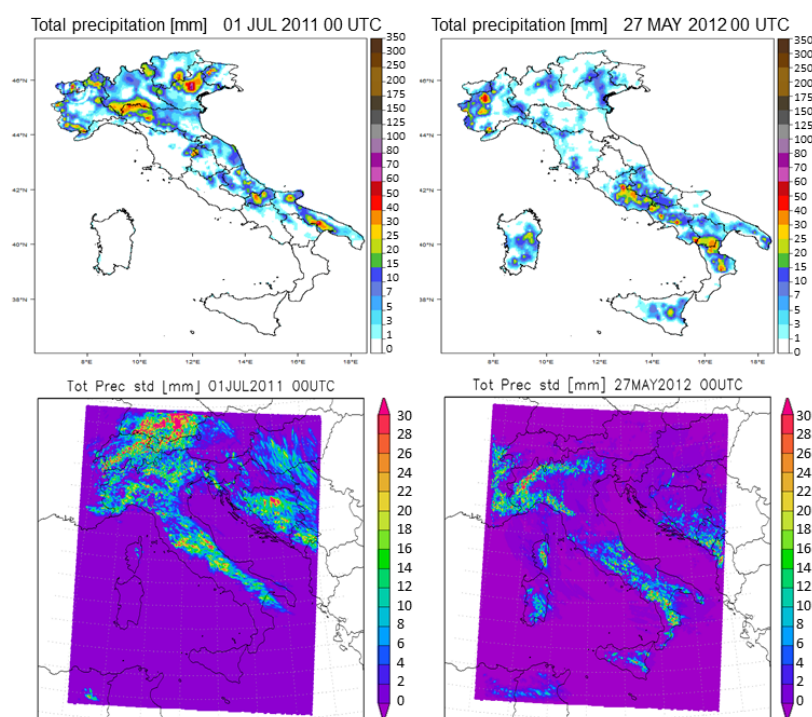


Figure 47: Total precipitation accumulated over 24 h (top row) and spread for this variable for the summer (left) and spring (right) cases.

This result indicates that the introduction of soil perturbation can add some skill to the ensemble system. Similar conclusion can be inferred considering the autumn case study, where the regions with the highest values of spread coincide with the regions of interesting weather (i.e. katabatic wind). In the winter case study, the spread increase is too weak and no noticeable signal can be detected. We investigated also if the different ICs of the soil have a contribution in the spread diffusion in the upper levels of the atmosphere. The spread of the main prognostic variables on longitudinal and latitudinal cross sections of the domain (Fig. 48), demonstrates that the soil moisture content change at the beginning of the simulations have a contribution in generating spread not only near the surface but even in the upper level of the atmosphere. In particular temperature spread is affected by the soil perturbation up to 850 hPa prognostic level, while the contribution to wind speed and water content spread propagates to higher levels affecting also the highest levels of the model integration. The speed of propagation of the spread in the upper atmosphere depends on the case study considered, because the phenomena involved in this study take place with

different time scales. The case studies associated with convective phenomena are the ones with the fastest spread propagation in the atmosphere. In the other cases, the propagation is slower and the spread diffuses less deeply in the upper levels of atmosphere.

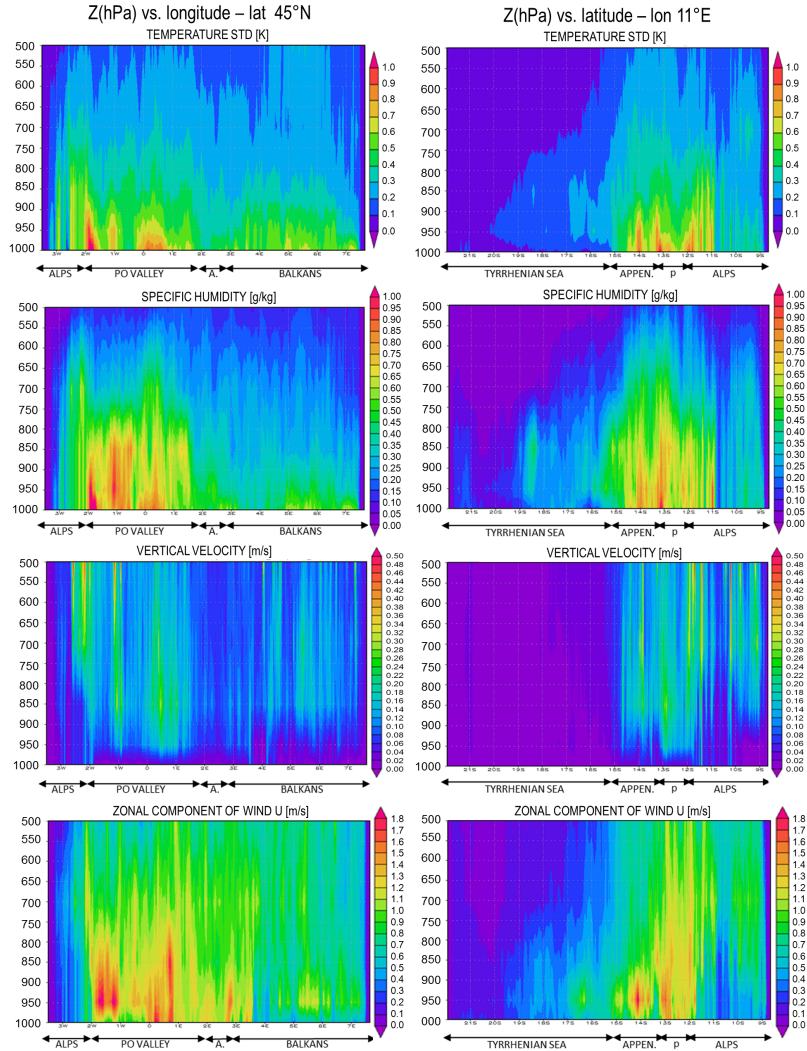


Figure 48: Spread of the main prognostic variables on longitudinal (left column) and latitudinal (right column) cross sections of the domain.

The results showed us that the model is very sensitive to soil moisture changes. This perturbation reflects in an increase of the spread of the main near-surface prognostic variables as well as upper in the atmosphere. The strength of the signal is higher in the case of convective case studies and weaker for the other cases. Moreover, in most of the analysed cases, it can be noticed that areas with large spread coincide with areas where “interesting” weather was observed, indicating that the soil moisture perturbation could potentially add some skill in the ensemble system. Considering the promising result of this study, we started the next phase of the priority project: test a perturbation technique in a full-fledged ensemble prediction system with ICs of soil and atmosphere as well as atmospheric BCs perturbed. Results of the sensitivity test are more extensively described in Bonanno and Loglisci (2014).

4.2.2 Implementing a soil perturbation technique in a high resolution ensemble system.

A first step to reach this goal was to choose between two available perturbation techniques. The first one (SHP hereafter, Spherical Harmonics Perturbation), proposed by Lavaysse et al. (2013), is based on perturbation of spectral coefficients in the expansion in spherical harmonics (in the horizontal) and Fourier harmonics (in the vertical). The second one (SPG hereafter, Stochastic Pattern Generator) is based on expansions in Fourier harmonics on a doubly periodic domain that contains the domain of interest (Tsyrlunikov and Gayfulin, 2016). This last SPG technique has been preferred because it gives a more irregular and noisy random field compared with the SHP technique. Moreover, SPG has the advantage of being less expensive from a computational point of view. Being SPG, with a specific setting, the selected technique to perturb soil field, we performed a sensitivity to initial soil moisture fields: the first coming from COSMO-EU (the operational run of DWD at the time of the experiments, with 7 km horizontal resolution over Europe), the second from the IFS model of ECMWF. This sensitivity test demonstrated that perturbing ECMWF initial soil moisture field gives a negative impact in terms of spread generation because of its highest values of soil moisture, close to saturation. To complete the sensitivity test, we tried to understand how sensitive the ensemble system is to the perturbation of other soil related external parameters such as LAI (Leaf Area Index), roughness length and vegetation cover. This last experiment revealed that the perturbations of external soil related parameters do not have a great impact on the generation of spread for 2-m temperature or soil moisture. The same results were obtained for other variables such as 2-m dew point, 10-m wind speed, precipitation, vertical velocity and soil temperature. Moreover, perturbing both the soil moisture and the external soil related parameters did not have a significant impact on the spread in the surface variables.

The selected perturbation method was, finally:

- SPG (Stochastic Pattern Generator), having the best numerical performances in terms of computational demands to compute the perturbed fields;
- Soil Moisture as the only field to be perturbed in the soil initial conditions, because perturbing other soil related external parameters and/or a combination of them do not produce enough spread compared to the one produced by soil moisture initial condition perturbation;
- Initial soil moisture field from the COSMOEU, because the use of ECMWF soil moisture analysis has a negative impact in terms of spread generation. Moreover, the use of COSMOEU soil moisture field guarantees, as an added value, that soil initial conditions come from the same modelling system.

The effects of an initial soil surface perturbation on surface prognostic variables have been analysed, but the soil initial perturbation have, indeed, an effect on the upper level atmosphere. In fact, latitude-height and longitude-height cross sections demonstrate how the soil moisture initial condition perturbation with SPG and the selected setting is able to propagate spread from the bottom layer to middle troposphere (Fig. 49).

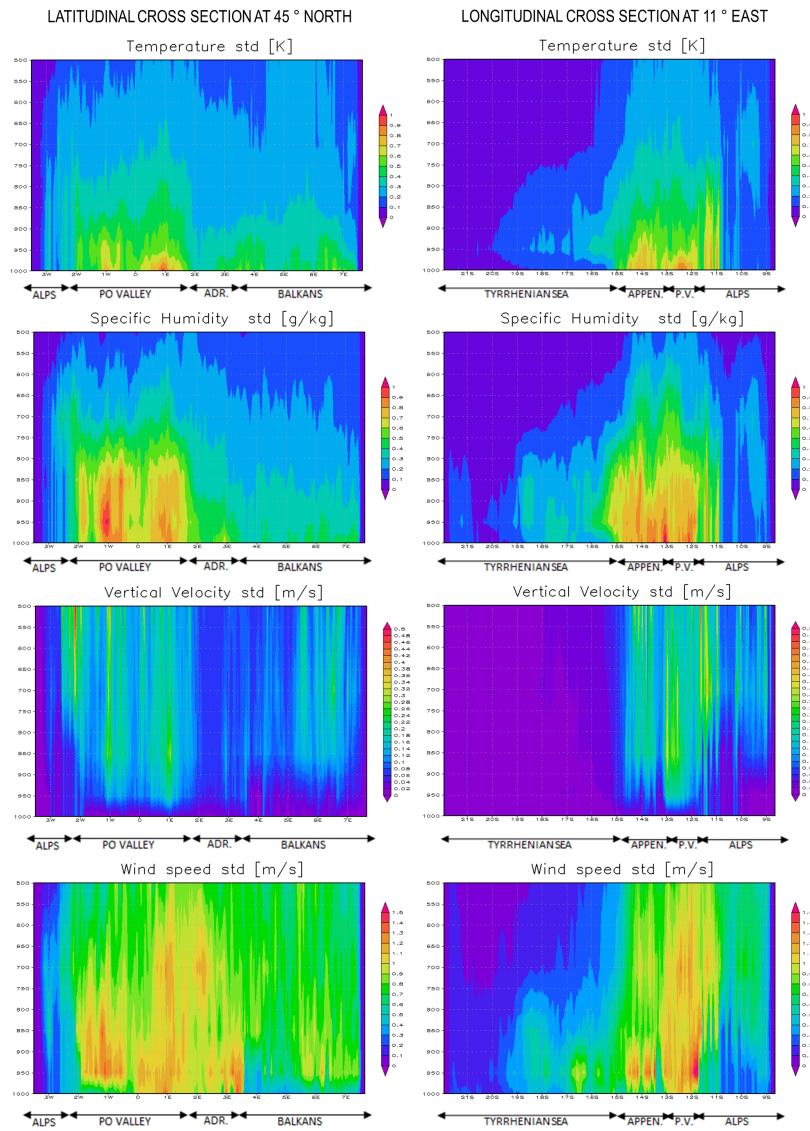


Figure 49: Spread of the main prognostic variables on longitudinal (left column) and latitudinal (right column) cross sections of the domain.

We finally compared the spread obtained with the selected soil perturbation technique with the one coming from an ensemble with perturbed atmospheric initial and boundary conditions, in this case COSMO-LEPS (Montani et al., 2011) (Fig. 50).

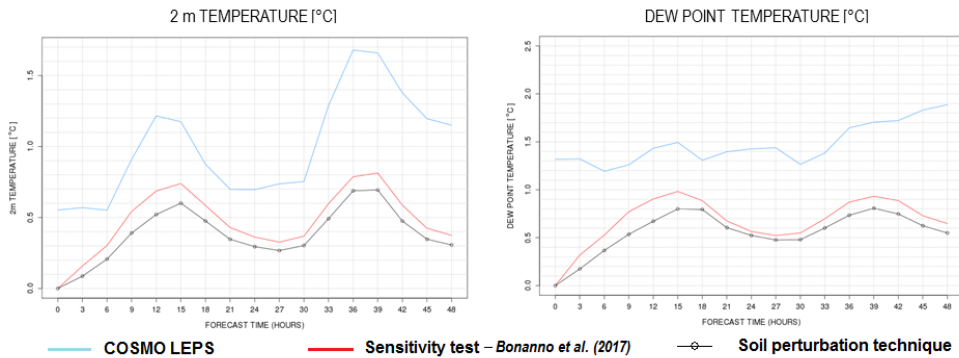


Figure 50: Spread of the variables indicated in panels averaged over the domain as a function of lead time, for the three systems COSMO-LEPS (blue line), a grouping of the runs performed in the sensitivity test (red line) and the ensemble generated by applying the soil perturbation technique based on SPG (black line).

Both systems produce comparable spreads as far as inland surface atmospheric variables are concerned. In fact, the main difference between the two EPSs is that COSMO-LEPS is able to produce spread also over the sea. Perturbing soil moisture initial condition has, naturally, a significant impact only for land areas. Over land the spread generated by the COSMO LEPS ensemble system is considerably higher than the one generated with the soil moisture perturbation. However, the latter is not negligible but gives a significant contribution, especially in the central hours of the day when the fluxes are higher. This fact led us to introduce the soil moisture perturbation into a full-fledged EPS expecting a positive contribution in term of spread generation. After this deep analysis, based on sensitivity of the model to soil uncertainties, we develop a perturbation technique able to generate randomly and numerically cheaply a perturbation of the soil moisture consistent with the model error of this important variable. This technique was successfully tested in a completely perturbed ensemble system based on the COSMO high resolution model, where perturbations act in the initial conditions of atmosphere and soil as well as in the boundary conditions of the atmosphere. Results have been published in COSMO Newsletter No. 15, Bonanno and Loglisci, 2015 and in a peer-reviewed paper (Bonanno and Loglisci, 2017).

5 References

- Bengtsson L., Steinheimer M., Bechtold P. and Geleyn J.-F., 2013: A stochastic parametrization for deep convection using cellular automata. *Quarterly Journal of the Royal Meteorological Society*, **139**, 675, 1533–1543.
- Berner J., Shutts G. J., Leutbecher M. and Palmer T. N., 2009: A spectral stochastic kinetic energy backscatter scheme and its impact on flow-dependent predictability in the ECMWF ensemble prediction system. *J. Atmos. Sci.*, **66**, 603–626.
- Berner J., Ha S.-Y., Hacker J. P., Fournier A. and Snyder C., 2011: Model Uncertainty in a Mesoscale Ensemble Prediction System: Stochastic versus Multiphysics Representations. *Mon. Wea. Rev.*, **139**, 1972–1995.
- Bonanno R. and Loglisci N., 2014: A sensitivity test to assess the impact of different soil moisture initializations on short range ensemble variability in COSMO model. COSMO Newsletter No. 14, available at <http://www.cosmo-model.org/content/model/documentation/newsLetters/default.htm>.

- Bonanno R. and Loglisci N., 2015: Setting up COSMO EPS perturbing lower boundary conditions: sensitivity and case studies. COSMO Newsletter No. 15, available at <http://www.cosmo-model.org/content/model/documentation/newsLetters/default.htm>.
- Bonanno R. and Loglisci N., 2018: Introducing lower boundary conditions perturbations in a convection-permitting ensemble system: sensitivity to soil moisture perturbation. *Meteorol. Atmos. Phys.*, **130**, 1, 67–80.
- Bowler N. E, Arribas A., Mylne K. R., Robertson K. B. and Beare S. E., 2008: The MOGREPS short-range ensemble prediction system. *Q. J. R. Meteorol. Soc.*, **134**, 703–722.
- Buizza R., Miller M. and Palmer, T. N., 1999: Stochastic simulation of model uncertainties. *Q. J. R. Meteorol. Soc.*, **125**, 2887–2908.
- Cloke H., Weisheimer A. and Pappenberger F., 2011: Representing uncertainty in land surface hydrology: fully coupled simulations with the ECMWF land surface scheme. Workshop on Model Uncertainty, 20-24 June 2011, ECMWF, Reading (UK).
- Doms G. and Baldauf M., 2015: A Description of the Nonhydrostatic COSMO-Model, Part I: Dynamics and Numerics. www.cosmo-model.org.
- Doms G., Förstner J., Heise E., Herzog H.-J., Mironov D., Raschendorfer M., Reinhardt T., Ritter B., Schrodin R., Schulz J.-P., Vogel G., 2011: A Description of the Nonhydrostatic Regional COSMO Model, Part II: Physical Parametrization. www.cosmo-model.org.
- Duniec G. and Mazur A., 2014: COTEKINO Priority Project - Results of Sensitivity Tests, COSMO Newsletter No. 14, 106-113.
- Duniec G., Interewicz W., Mazur A and Wyszogrodzki A., 2017: Operational Setup of the Soil-perturbed, Time-lagged Ensemble Prediction System at the Institute of Meteorology and Water Management - National Research Institute. *Meteorol. Hydrol. Water Manage.*, **5**, 2, 43–51.
- Gebhardt C., Theis S., Paulat M., Ben Bouallegue Z., 2011: Uncertainties in COSMO-DE precipitation forecasts introduced by model perturbations and variation of lateral boundaries. *Atmospheric Research*, **100**, Issues 2-3, 168–177.
- Hacker J. P., 2010: Spatial and temporal scales of boundary layer wind predictability in response to small-amplitude land surface uncertainty. *Journal of the Atmospheric Sciences*, **67**, 217–233.
- Jolliffe I.P. and Stephenson D.B., 2011: Forecast Verification: A Practitioner’s Guide in Atmospheric Science. Chapter 8 (Weigel, A.P.): Verification of Ensemble Forecast. Wiley.
- Lavaysse C. M., Carrera S., Bélair N., Gagnon R., Frenette M., Charron M. and Yau M. K., 2013: Impact of surface parameter uncertainties within the Canadian Regional Ensemble Prediction System. *Mon. Wea. Rev.*, **141**, 1506–1526.
- Marsigli C., 2009: COSMO-SREPS Priority Project ”Short Range Ensemble Prediction System (SREPS): final report. COSMO Technical Report No 13.
- Marsigli C., Montani A. and Paccagnella T., 2014: Provision of boundary conditions for a convection-permitting ensemble: comparison of two different approaches. *Nonlin. Processes Geophys.*, **21**, 393–403.
- Maurer D., Walser A. and Arpagaus M., 2014: First COSMO-E Experiments with the Stochastically Perturbed Parametrization Tendencies (SPPT) Scheme, COSMO Newsletter No. 14, available at

<http://www.cosmo-model.org/content/model/documentation/newsLetters/newsLetter14/>.

Mazur A. and Duniec G., 2014a: Sensitivity test on the behaviour of different COSMO suites to different lower boundary initial conditions. Presented during COSMO User Seminar, 16-21.03.2014, Offenbach, Germany.

Mazur A. and Duniec G., 2014b: Soil state perturbations as an input for Ensemble Prediction System (EPS) forecast, Side, Antalya/Turkey, 14-16 October, 2014, Turkey.

Mazur A. and Duniec G., 2015: Ensemble Prediction System (EPS)-based forecast prepared from perturbations of soil conditions, COSMO Newsletter No. 15.

Montani A., Cesari D., Marsigli C. and Paccagnella T., 2011: Seven years of activity in the field of mesoscale ensemble forecasting by the COSMO-LEPS system: main achievements and open challenges. *Tellus A*, **63**, 605–624.

Montani A., Marsigli C. and Paccagnella T., 2013: Development of a COSMO-based limited-area ensemble system for the 2014 Winter Olympic Games. COSMO Newsletter, No. 13, 9399. Available online at http://cosmo-model.org/content/model/documentation/newsLetters/newsLetter13/cnl13_12.pdf.

Montani A., Alferov D., Astakhova E., Marsigli C. and Paccagnella T., 2014: Ensemble forecasting for Sochi-2014 Olympics: the COSMO-based ensemble prediction systems. COSMO Newsletter, No. 14, 8894. Available online at http://cosmo-model.org/content/model/documentation/newsLetters/newsLetter14/cnl14_10.pdf.

Palmer T. N., Buizza R., Doblas-Reyes F., Jung T., Leutbecher M., Shutts G. J., Steinheimer M. and Weisheimer A., 2009: Stochastic parametrization and model uncertainty. ECMWF Research Department Technical Memorandum n. 598, ECMWF, Shinfield Park, Reading RG2-9AX, UK, pp. 42.

Peralta C., Ben Bouallegue Z., Theis S., Gebhardt C. and Buchhold M., 2012: Accounting for initial condition uncertainties in COSMO-DE-EPS. *Journal of Geophysical Research: Atmospheres*, **117**, D7, 1–13.

Plant R. S. and Craig G. C., 2008: A Stochastic Parametrization for Deep Convection Based on Equilibrium Statistics. *Journal of the Atmospheric Sciences*, **65**, 87–105.

Rüdisühli S., Walser A., and Fuhrer O., 2014: COSMO in Single Precision, COSMO Newsletter No. 14, available at <http://www.cosmo-model.org/content/model/documentation/newsLetters/newsLetter14/>.

Schättler U., Doms G. and Schraff C., 2016: A Description of the Nonhydrostatic COSMO-Model, Part VII: Users Guide, www.cosmo-model.org.

Shutts G., 2005: A kinetic energy backscatter algorithm for use in ensemble prediction systems. *Q. J. R. Meteorol. Soc.*, **131**, 3079–3102.

Sutton C.J. and Hamill T.M., 2004: Impacts of perturbed soil moisture conditions on short range ensemble variability. 84th AMS Annual Meeting, 20th Conference on Weather Analysis and Forecasting/16th Conference on Numerical Weather Prediction, 12-15 January 2004, Seattle, WA.

Sutton C., Hamill T. and Warner T., 2006: Will perturbing soil moisture improve warm-season ensemble forecasts? A proof of concept. *Mon. Weather Rev.*, **134**, 3174–3189.

Tsyrlunikov M. and D. Gayfulin D., 2016: A Stochastic Pattern Generator for ensemble applications. COSMO Technical Report No. 29, available at [www.cosmo-model.org /con-](http://www.cosmo-model.org/content/)

tent/model/documentation/techReports/default.htm.

Vié B., Nuissier O. and Ducroucq V., 2011: Cloud-resolving ensemble simulations of Mediterranean heavy precipitating events: uncertainty on initial conditions and lateral boundary conditions. *Monthly Weather Review*, **139**, 403–423.

Wang Y., Kann A., Bellus M., Pailleux J. and Wittmann C., 2010: A strategy for perturbing surface conditions in LAMEPS, *Atmos Sci Lett*, **11**, 108–113.

List of COSMO Newsletters and Technical Reports

(available for download from the COSMO Website: www.cosmo-model.org)

COSMO Newsletters

- No. 1: February 2001.
- No. 2: February 2002.
- No. 3: February 2003.
- No. 4: February 2004.
- No. 5: April 2005.
- No. 6: July 2006.
- No. 7: April 2008; Proceedings from the 8th COSMO General Meeting in Bucharest, 2006.
- No. 8: September 2008; Proceedings from the 9th COSMO General Meeting in Athens, 2007.
- No. 9: December 2008.
- No. 10: March 2010.
- No. 11: April 2011.
- No. 12: April 2012.
- No. 13: April 2013.
- No. 14: April 2014.
- No. 15: July 2015.
- No. 16: July 2016.
- No. 17: July 2017.

COSMO Technical Reports

- No. 1: Dmitrii Mironov and Matthias Raschendorfer (2001):
Evaluation of Empirical Parameters of the New LM Surface-Layer Parameterization Scheme. Results from Numerical Experiments Including the Soil Moisture Analysis.
- No. 2: Reinhold Schrodin and Erdmann Heise (2001):
The Multi-Layer Version of the DWD Soil Model TERRA_LM.
- No. 3: Günther Doms (2001):
A Scheme for Monotonic Numerical Diffusion in the LM.
- No. 4: Hans-Joachim Herzog, Ursula Schubert, Gerd Vogel, Adelheid Fiedler and Roswitha Kirchner (2002):
LLM - the High-Resolving Nonhydrostatic Simulation Model in the DWD-Project LIT-FASS.
Part I: Modelling Technique and Simulation Method.

- No. 5: Jean-Marie Bettems (2002):
EUCOS Impact Study Using the Limited-Area Non-Hydrostatic NWP Model in Operational Use at MeteoSwiss.
- No. 6: Heinz-Werner Bitzer and Jürgen Steppeler (2004):
Documentation of the Z-Coordinate Dynamical Core of LM.
- No. 7: Hans-Joachim Herzog, Almut Gassmann (2005):
Lorenz- and Charney-Phillips vertical grid experimentation using a compressible non-hydrostatic toy-model relevant to the fast-mode part of the 'Lokal-Modell'.
- No. 8: Chiara Marsigli, Andrea Montani, Tiziana Paccagnella, Davide Sacchetti, André Walser, Marco Arpagaus, Thomas Schumann (2005):
Evaluation of the Performance of the COSMO-LEPS System.
- No. 9: Erdmann Heise, Bodo Ritter, Reinhold Schrodin (2006):
Operational Implementation of the Multilayer Soil Model.
- No. 10: M.D. Tsyrlunikov (2007):
Is the particle filtering approach appropriate for meso-scale data assimilation ?
- No. 11: Dmitrii V. Mironov (2008):
Parameterization of Lakes in Numerical Weather Prediction. Description of a Lake Model.
- No. 12: Adriano Raspanti (2009):
COSMO Priority Project "VERification System Unified Survey" (VERSUS): Final Report.
- No. 13: Chiara Marsigli (2009):
COSMO Priority Project "Short Range Ensemble Prediction System" (SREPS): Final Report.
- No. 14: Michael Baldauf (2009):
COSMO Priority Project "Further Developments of the Runge-Kutta Time Integration Scheme" (RK): Final Report.
- No. 15: Silke Dierer (2009):
COSMO Priority Project "Tackle deficiencies in quantitative precipitation forecast" (QPF): Final Report.
- No. 16: Pierre Eckert (2009):
COSMO Priority Project "INTERP": Final Report.
- No. 17: D. Leuenberger, M. Stoll and A. Roches (2010):
Description of some convective indices implemented in the COSMO model.
- No. 18: Daniel Leuenberger (2010):
Statistical analysis of high-resolution COSMO Ensemble forecasts in view of Data Assimilation.
- No. 19: A. Montani, D. Cesari, C. Marsigli, T. Paccagnella (2010):
Seven years of activity in the field of mesoscale ensemble forecasting by the COSMO-LEPS system: main achievements and open challenges.
- No. 20: A. Roches, O. Fuhrer (2012):
Tracer module in the COSMO model.

- No. 21: Michael Baldauf (2013):
A new fast-waves solver for the Runge-Kutta dynamical core.
- No. 22: C. Marsigli, T. Diomede, A. Montani, T. Paccagnella, P. Louka, F. Gofa, A. Corigliano (2013):
The CONSENS Priority Project.
- No. 23: M. Baldauf, O. Fuhrer, M. J. Kurowski, G. de Morsier, M. Müllner, Z. P. Piotrowski, B. Rosa, P. L. Vitagliano, D. Wójcik, M. Ziemiański (2013):
The COSMO Priority Project 'Conservative Dynamical Core' Final Report.
- No. 24: A. K. Miltenberger, A. Roches, S. Pfahl, H. Wernli (2014):
Online Trajectory Module in COSMO: a short user guide.
- No. 25: P. Khain, I. Carmona, A. Voudouri, E. Avgoustoglou, J.-M. Bettems, F. Grazzini (2015):
The Proof of the Parameters Calibration Method: CALMO Progress Report.
- No. 26: D. Mironov, E. Machulskaya, B. Szintai, M. Raschendorfer, V. Perov, M. Chumakov, E. Avgoustoglou (2015):
The COSMO Priority Project 'UTCS' Final Report.
- No. 27: J.-M. Bettems (2015):
The COSMO Priority Project 'COLOBOC': Final Report.
- No. 28: Ulrich Blahak (2016):
RADAR_MIE_LM and RADAR_MIELIB - Calculation of Radar Reflectivity from Model Output.
- No. 29: M. Tsyrlunikov and D. Gayfulin (2016):
A Stochastic Pattern Generator for ensemble applications.
- No. 30: D. Mironov and E. Machulskaya (2017):
A Turbulence Kinetic Energy – Scalar Variance Turbulence Parameterization Scheme.
- No. 31: P. Khain, I. Carmona, A. Voudouri, E. Avgoustoglou, J.-M. Bettems, F. Grazzini, P. Kaufmann (2017):
CALMO - Progress Report.
- No. 32: A. Voudouri, P. Khain, I. Carmona, E. Avgoustoglou, J.M. Bettems, F. Grazzini, O. Bellprat, P. Kaufmann and E. Bucchignani (2017):
Calibration of COSMO Model, Priority Project CALMO Final report
- No. 33: N. Vela (2017):
VAST 2.0 - User Manual.

COSMO Technical Reports

Issues of the COSMO Technical Reports series are published by the *COnsortium for Small-scale MOdelling* at non-regular intervals. COSMO is a European group for numerical weather prediction with participating meteorological services from Germany (DWD, AWGeophys), Greece (HNMS), Italy (USAM, ARPA-SIMC, ARPA Piemonte), Switzerland (MeteoSwiss), Poland (IMGW), Romania (NMA) and Russia (RHM). The general goal is to develop, improve and maintain a non-hydrostatic limited area modelling system to be used for both operational and research applications by the members of COSMO. This system is initially based on the COSMO-Model (previously known as LM) of DWD with its corresponding data assimilation system.

The Technical Reports are intended

- for scientific contributions and a documentation of research activities,
- to present and discuss results obtained from the model system,
- to present and discuss verification results and interpretation methods,
- for a documentation of technical changes to the model system,
- to give an overview of new components of the model system.

The purpose of these reports is to communicate results, changes and progress related to the LM model system relatively fast within the COSMO consortium, and also to inform other NWP groups on our current research activities. In this way the discussion on a specific topic can be stimulated at an early stage. In order to publish a report very soon after the completion of the manuscript, we have decided to omit a thorough reviewing procedure and only a rough check is done by the editors and a third reviewer. We apologize for typographical and other errors or inconsistencies which may still be present.

At present, the Technical Reports are available for download from the COSMO web site (www.cosmo-model.org). If required, the member meteorological centres can produce hardcopies by their own for distribution within their service. All members of the consortium will be informed about new issues by email.

For any comments and questions, please contact the editor:

Massimo Milelli
Massimo.Milelli@arpa.piemonte.it